Ribosomal RNA (rRNA) sequences from 33 globally distributed mosquito species for improved metagenomics and species identification

Cassandra Koh, Lionel Frangeul, Hervé Blanc, Carine Ngoagouni, Sébastien Boyer, Philippe Dussart, Nina Grau, Romain Girod, Jean-Bernard Duchemin, Maria-Carla Saleh

Ribosomal RNA (rRNA) sequences from 33 globally distributed mosquito species for improved metagenomics and species identification

Cassandra Koh[1*], Lionel Frangeul[1], Hervé Blanc[1], Carine Ngoagouni[2], Sébastien Boyer[3], Philippe Dussart[4], Nina Grau[5], Romain Girod[5], Jean-Bernard Duchemin[6] and Maria-Carla Saleh[1*]

[1] Viruses and RNA Interference Unit, Institut Pasteur, Université Paris Cité, CNRS UMR3569, Paris F-75015, France

[2] Medical Entomology Laboratory, Institut Pasteur de Bangui, Bangui PO Box 923, Central African Republic

[3] Medical and Veterinary Entomology Unit, Institut Pasteur du Cambodge, Phnom Penh 12201, Cambodia

[4] Virology Unit, Institut Pasteur du Cambodge, Phnom Penh 12201, Cambodia

[5] Medical Entomology Unit, Institut Pasteur de Madagascar, Antananarivo 101, Madagascar

[6] Vectopôle Amazonien Emile Abonnenc, Institut Pasteur de la Guyane, Cayenne 97306, French Guiana

* To whom correspondence should be addressed.

Present address: Philippe Dussart, Institut Pasteur de Madagascar, Antananarivo 101, Madagascar; Nina Grau, Sciences Economiques et Sociales de la Santé et Traitement de l'Information Médicale, Faculté de Médecine, Marseille 13005, France

Corresponding authors: Cassandra Koh, cassandra.koh@pasteur.fr, +33 1 40 61 36 74; Maria-Carla Saleh, carla.saleh@pasteur.fr, +33 1 45 68 85 47.

ABSTRACT

Total RNA sequencing (RNA-seq) is an important tool in the study of mosquitoes and the RNA viruses they vector as it allows assessment of both host and viral RNA in specimens. However, there are two main constraints. First, as with many other species, abundant mosquito ribosomal RNA (rRNA) serves as the predominant template from which sequences are generated, meaning that the desired host and viral templates are sequenced far less. Second, mosquito specimens captured in the field must be correctly identified, in some cases to the sub-species level. Here, we generate mosquito ribosomal RNA (rRNA) datasets which will substantially mitigate both of these problems. We describe a strategy to assemble novel rRNA sequences from mosquito specimens and produce an unprecedented dataset of 234 full-length 28S and 18S rRNA sequences of 33 medically important species from countries with known histories of mosquito-borne virus circulation (Cambodia, the Central African Republic, Madagascar, and French Guiana). These sequences will allow both physical and computational removal of rRNA from specimens during RNAseq protocols. We also assess the utility of rRNA sequences for molecular taxonomy and compare phylogenies constructed using rRNA sequences versus those created using the gold standard for molecular species identification of specimens—the mitochondrial *cytochrome* c *oxidase I* (COI) gene. We find that rRNA- and COI-derived phylogenetic trees are incongruent and that 28S and concatenated 28S+18S rRNA phylogenies reflect evolutionary relationships that are more aligned with contemporary mosquito systematics. This significant expansion to the current rRNA reference library for mosquitoes will improve mosquito RNA-seq metagenomics by permitting the optimization of species-specific rRNA depletion protocols for a broader range of species and streamlining species identification by rRNA sequence and phylogenetics.

Keywords: surveillance, RNA-seq, ribosomal RNA, molecular marker, metagenomics, mosquito

INTRODUCTION

Mosquitoes top the list of vectors for arthropod-borne diseases, being implicated in the transmission of many human pathogens responsible for arboviral diseases, malaria, and lymphatic filariasis (WHO, 2017). Mosquito-borne viruses circulate in sylvatic (between wild animals) or urban (between humans) transmission cycles driven by different mosquito species with their own distinct host preferences. Although urban mosquito species are chiefly responsible for amplifying epidemics in dense human populations, sylvatic mosquitoes maintain the transmission of these viruses among forest-dwelling animal reservoir hosts and are implicated in spillover events when humans enter their ecological niches (Valentine et al., 2019). Given that mosquito-borne virus emergence is preceded by such spillover events, continuous surveillance and virus discovery in sylvatic mosquitoes is integral to designing effective public health measures to pre-empt or respond to mosquito-borne viral epidemics.

Metagenomics on field specimens is the most powerful method in the toolkit for understanding mosquito-borne disease ecology through the One Health lens (Webster et al., 2016). With next-generation sequencing becoming more accessible, such studies have provided unprecedented insights into the interfaces among mosquitoes, their environment, and their animal and human hosts. As mosquito-associated viruses are mostly RNA viruses, RNA sequencing (RNA-seq) is especially informative for surveillance and virus discovery. However, working with lesser studied mosquito species poses several problems.

First, metagenomics studies based on RNA-seq are bedevilled by overabundant ribosomal RNAs (rRNAs). These non-coding RNA molecules comprise at least 80% of the total cellular RNA population (Gale & Crampton, 1989). Due to their length and their abundance, they are a sink for precious next generation sequencing reads, decreasing the sensitivity of pathogen detection unless depleted during library preparation. Yet the most common rRNA depletion protocols require prior knowledge of rRNA sequences of the species of interest as they involve hybridizing antisense oligos to the rRNA molecules prior to removal by ribonucleases (Fauver et al., 2019; Phelps et al., 2021) or by bead capture (Kukutla et al., 2013). Presently, reference sequences for rRNAs are limited to only a handful of species from three genera: *Aedes*, *Culex*, and *Anopheles* (Ruzzante et al., 2019). The lack of reliable rRNA depletion methods could deter mosquito metagenomics studies from expanding their sampling diversity, resulting in a gap in our knowledge of mosquito vector ecology. The inclusion of lesser studied yet medically relevant sylvatic species is therefore imperative.

Second, species identification based on morphology is notoriously complicated for members of species subgroups. This is especially the case among *Culex* subgroups. Sister species are often sympatric and show at least some competence for a number of viruses, such as Japanese encephalitis virus, St Louis encephalitic virus, and Usutu virus (Nchoutpouen et al., 2019). Although they share many morphological traits, each of these species have distinct ecologies and host preferences, thus the challenge of correctly identifying vector species can affect epidemiological risk estimation for these diseases (Farajollahi et al., 2011). DNA molecular markers are often employed to a limited degree of success to distinguish between sister species (Batovska et al., 2017; Zittra et al., 2016).

To address the lack of full-length rRNA sequences in public databases, we sought to determine the 28S and 18S rRNA sequences of a diverse set of Old and New World sylvatic mosquito species from four countries representing three continents: Cambodia, the Central African Republic, Madagascar, and French Guiana. These countries, due to their proximity to the equator, contain high mosquito biodiversity (Foley et al., 2007) and have had long histories of mosquito-borne virus circulation (Desdouits et al., 2015; Halstead, 2019; Héraud et al., 2022; Jacobi & Serie, 1972; Ratsitorahina et al., 2008; Saluzzo et al., 2018; Zeller et al., 2016). Increased and continued surveillance of local mosquito species could lead to valuable insights on mosquito virus biogeography. Using a unique score-based read filtration strategy to remove interfering non-mosquito rRNA reads for accurate *de novo* assembly, we produced a dataset of 234 novel full-length 28S and 18S rRNA sequences from 33 mosquito species, 30 of which have never been recorded before.

We also explored the functionality of 28S and 18S rRNA sequences as molecular markers by comparing their performance to that of the mitochondrial *cytochrome* c *oxidase subunit I* (COI) gene for molecular taxonomic and phylogenetic investigations. The COI gene is the most widely used DNA marker for molecular species identification and forms the basis of the Barcode of Life Data System (BOLD) (Hebert et al., 2003; Ratnasingham & Hebert, 2007). Presently, full-length rRNA sequences are much less represented compared to other molecular markers. However, given the availability of relevant reference sequences, 28S and concatenated 28S+18S rRNA sequences can be the better approach for molecular taxonomy and phylogenetic studies. We hope that our sequence dataset, with its species diversity and eco-geographical breadth, and the assembly strategy we describe would further facilitate the use of rRNA as markers. In addition, this dataset enables the design of species-

specific oligos for cost-effective rRNA depletion for a broader range of mosquito species and streamlined molecular species identification during RNA-seq.

RESULTS

Poor rRNA depletion using a non-specific depletion method

During library preparations of mosquito samples for RNA-seq, routinely used methods for depleting rRNA are commercial kits optimised for human or mice samples (Belda et al., 2019; Bishop-Lilly et al., 2010; Chandler et al., 2015; N. Kumar et al., 2012; Weedall et al., 2015; Zakrzewski et al., 2018) or through 80–100 base pair antisense probe hybridisation followed by ribonuclease digestion (Fauver et al., 2019; Phelps et al., 2021). In cases where the complete reference rRNA sequence of the target species is not known, oligos would be designed based on the rRNA sequence of the closest related species (25, this study). These methods should deplete the conserved regions of rRNA sequences. However, the variable regions remain at abundances high enough to compromise RNA-seq output. In our hands, we have found that using probes designed for the *Ae. aegypti* rRNA sequence followed by RNase H digestion according to the protocol published by Morlan *et al.* (2012) produced poor depletion in *Ae. albopictus*, and in Culicine and Anopheline species (Figure 1), in which between 46–94% of reads post-depletion were ribosomal. Additionally, the lack of reference rRNA sequences compromises the *in silico* clean-up of remaining rRNA reads from sequencing data, as reads belonging to variable regions would not be removed. To solve this and to enable RNA-seq metagenomics on a broader range of mosquito species, we performed RNA-seq to generate reference rRNA sequences for 33 mosquito species representing 10 genera from Cambodia, the Central African Republic, Madagascar, and French Guiana. Most of these species are associated with vector activity for various pathogens in their respective ecologies (Table 1). In parallel, we sequenced the mitochondrial COI gene to perform molecular species identification of our samples and to comparatively evaluate the use of rRNA as a molecular marker (Figure 2).

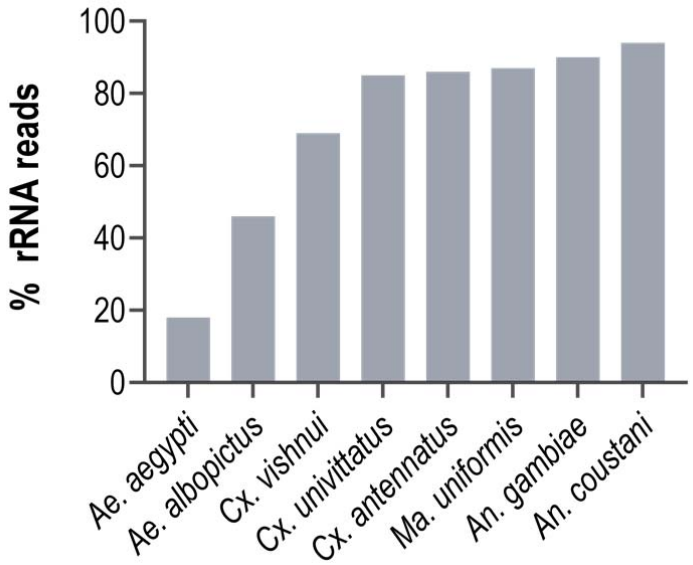

129

130 **Figure 1. Percentage of rRNA reads in mosquito total RNA-seq data after depletion using**
131 **probes antisense to *Ae. aegypti* sequences.** Pools of 5 individual mosquitoes were ribodepleted by
132 probe hybridisation followed by RNase H digestion according to the protocol by Morlan *et al.* (2012).
133 Percentages of remaining rRNA reads were calculated from the number of rRNA reads over total
134 reads per sample pool. Depletion efficiency decreases with taxonomic distance from *Ae. aegypti*
135 underlining the need for reference sequences for species of interest.

136 **Table 1.** Mosquito species represented in this study and their vector status.

Mosquito taxonomy*	Origin**	Collection site (ecosystem type)	Vector for***	Reference
Aedes (Fredardsius) vittatus	CF	rural (village)	ZIKV, CHIKV, YFV	(Diallo et al., 2020)
Aedes (Ochlerotatus) scapularis	GF	rural (village)	YFV	(Vasconcelos et al., 2001)
Aedes (Ochlerotatus) serratus	GF	rural (village)	YFV, OROV	(Cardoso et al., 2010; Romero-Alvarez & Escobar, 2018)
Aedes (Stegomyia) aegypti	CF	urban	DENV, ZIKV, CHIKV, YFV	(Kraemer et al., 2019)
Aedes (Stegomyia) albopictus	CF, KH	rural (village, nature reserve)	DENV, ZIKV, CHIKV, YFV, JEV	(Auerswald et al., 2021; Kraemer et al., 2019)
Aedes (Stegomyia) simpsoni	CF	rural (village)	YFV	(Mukwaya et al., 2000)
Anopheles (Anopheles) baezai	KH	rural (nature reserve)	unreported	–
Anopheles (Anopheles) coustani	MG, CF	rural (village)	RVFV, malaria	(Mwangangi et al., 2013; Nepomichene et al., 2018; Ratovonjato et al., 2011)
Anopheles (Cellia) funestus	MG, CF	rural (village)	ONNV, malaria	(Lutomiah et al., 2013; Tabue et al., 2017)
Anopheles (Cellia) gambiae	MG, CF	rural (village)	ONNV, malaria	(Brault et al., 2004)
Anopheles (Cellia) squamosus	MG	rural (village)	RVFV, malaria	(Ratovonjato et al., 2011; Stevenson et al., 2016)

Coquillettidia (Rhynchotaenia) venezuelensis	GF	rural (village)	OROV	(Travassos Da Rosa et al., 2017)
Culex (Culex) antennatus	MG	rural (village)	RVFV	(Nepomichene et al., 2018; Ratovonjato et al., 2011)
Culex (Culex) duttoni	CF	rural (village)	unreported	–
Culex (Culex) neavei	MG	rural (village)	USUV	(Nikolay et al., 2011)
Culex (Culex) orientalis	KH	rural (nature reserve)	JEV	(Kim et al., 2015)
Culex (Culex) perexiguus	MG	rural (village)	WNV, USUV	(Vázquez González et al., 2011)
Culex (Culex) pseudovishnui	KH	rural (nature reserve)	JEV	(Auerswald et al., 2021)
Culex (Culex) quinquefasciatus	MG, CF, KH	rural (village, nature reserve)	ZIKV, JEV, WNV, DENV, SLEV, RVFV, *Wuchereria bancrofti*	(Bhattacharya & Basu, 2016; Maquart et al., 2021; Ndiaye et al., 2016; Pereira Serra et al., 2016)
Culex (Culex) tritaeniorhynchus	MG, KH	rural (village, nature reserve)	JEV, WNV, RVFV	(Auerswald et al., 2021; Hayes et al., 1980; Jupp et al., 2002)
Culex (Melanoconion) spissipes	GF	rural (village)	VEEV	(Weaver et al., 2004)
Culex (Melanoconion) portesi	GF	rural (village)	VEEV, TONV	(Talaga et al., 2021; Weaver et al., 2004)
Culex (Melanoconion) pedroi	GF	rural (village)	EEEV, VEEV, MADV	(Talaga et al., 2021; M. J. Turell et al., 2008)
Culex (Oculeomyia) bitaeniorhynchus	MG, KH	rural (village, nature reserve)	JEV	(Auerswald et al., 2021)
Culex (Oculeomyia) poicilipes	MG	rural (village)	RVFV	(Ndiaye et al., 2016)
Eretmapodites intermedius	CF	rural (village)	unreported	–
Limatus durhamii	GF	rural (village)	ZIKV	(Barrio-Nuevo et al., 2020)
Mansonia (Mansonia) titillans	GF	rural (village)	VEEV, SLEV	(Hoyos-López et al., 2015; Michael J Turell, 1999)
Mansonia (Mansonioides) indiana	KH	rural (nature reserve)	JEV	(Arunachalam et al., 2004)
Mansonia (Mansonioides) uniformis	MG, CF, KH	rural (village, nature reserve)	RVFV, *Wuchereria bancrofti*	(Lutomiah et al., 2013; Ughasi et al., 2012)
Mimomyia (Etorleptiomyia) mediolineata	MG	rural (village)	unreported	–
Psorophora (Janthinosoma) ferox	GF	rural (village)	ROCV	(Mitchell et al., 1986)
Uranotaenia (Uranotaenia) geometrica	GF	rural (village)	unreported	–

* () indicates subgenus

** Origin countries are listed as their ISO alpha-2 codes: Central African Republic, CF; Cambodia, KH; Madagascar, MG; French Guiana, GF.

** dengue virus, DENV; Zika virus, ZIKV; chikungunya virus, CHIKV; Yellow Fever virus, YFV; Oropouche virus, OROV; Japanese encephalitis virus, JEV; Rift Valley Fever virus, RVFV; O'Nyong Nyong virus, ONNV; Usutu virus, USUV; West Nile virus, WNV; Saint Louis encephalitis virus, SLEV; Venezuelan equine encephalitis virus, VEEV; Tonate virus, TONV; Eastern equine encephalitis virus, EEEV; Madariaga virus, MADV; Rocio virus, ROCV.

rRNA reads filtering and sequence assembly

Assembling Illumina reads to reconstruct rRNA sequences from total mosquito RNA is not a straightforward task. Apart from host rRNA, total RNA samples also contain rRNA from other

organisms associated with the host (microbiota, external parasites, or ingested diet). As rRNA sequences share high homology in conserved regions, Illumina reads (150 bp) from non-host rRNA can interfere with the contig assembly of host 28S and 18S rRNA.

Our score-based filtration strategy, described in detail in the Methods section, allowed us to bioinformatically remove interfering rRNA reads and achieve successful *de novo* assembly of 28S and 18S rRNA sequences for all our specimens. Briefly, for each Illumina read, we computed a ratio of BLAST scores against an Insecta library over scores against a Non-Insecta library (Figure 2A). Based on their ratio of scores, reads could be segregated into four categories (Figure 2B): (i) reads mapping only to the Insecta library, (ii) reads mapping better to the Insecta relative to Non-Insecta library, (iii) reads mapping better to the Non-Insecta relative to the Insecta library, and (iv) reads mapping only to the Non-Insecta library. By applying a conservative threshold at 0.8 to account for the non-exhaustiveness of the SILVA database, we removed reads that likely do not originate from mosquito rRNA. Notably, 15 of our specimens were engorged with vertebrate blood, a rich source of non-mosquito rRNA (Appendix 1—table 1). The successful assembly of complete 28S and 18S rRNA sequences for these specimens demonstrates that this strategy performs as expected even with high amounts of non-host rRNA reads. This is particularly important in studies on field-captured mosquitoes as females are often sampled already having imbibed a blood meal or captured using the human landing catch technique.

We encountered challenges for three specimens morphologically identified as *Ma. africana* (Specimen ID S33–S35) (Appendix 1—table 1). COI amplification by PCR did not produce any product, hence COI sequencing could not be used to confirm species identity. In addition, the genome assembler SPAdes (Bankevich et al., 2012) was only able to assemble partial length rRNA contigs, despite the high number of reads with high scores against the Insecta library. Among other *Mansonia* specimens, the partial length contigs shared the highest similarity with contigs obtained from sample “Ma uniformis CF S51”. We then performed a guided assembly using the 28S and 18S sequences of this specimen as references, which successfully produced full-length contigs. In two of these specimens (Specimen ID S34 and S35), our assembly initially produced two sets of 28S and 18S rRNA sequences, one of which was similar to mosquito rRNA with low coverage and another with ten-fold higher coverage and 95% nucleotide sequence similarity to a water mite of genus *Horreolanus* known to parasitize mosquitoes. Our success in obtaining rRNA sequences for mosquito and water

178 mite shows that our strategy can be applied to metabarcoding studies where the input material
179 comprises multiple insect species, provided that appropriate reference sequences of the target
180 species or of a close relative are available.
181 Altogether, we were able to assemble 122 28S and 114 18S full-length rRNA sequences for 33
182 mosquito species representing 10 genera sampled from four countries across three continents. This
183 dataset contains, to our knowledge, the first records for 30 mosquito species and for seven genera:
184 *Coquillettidia*, *Mansonia*, *Limatus*, *Mimomyia*, *Uranotaenia*, *Psorophora,* and *Eretmapodites*.
185 Individual GenBank accession numbers for these sequences and specimen information are listed in
186 Appendix 1—table 1.

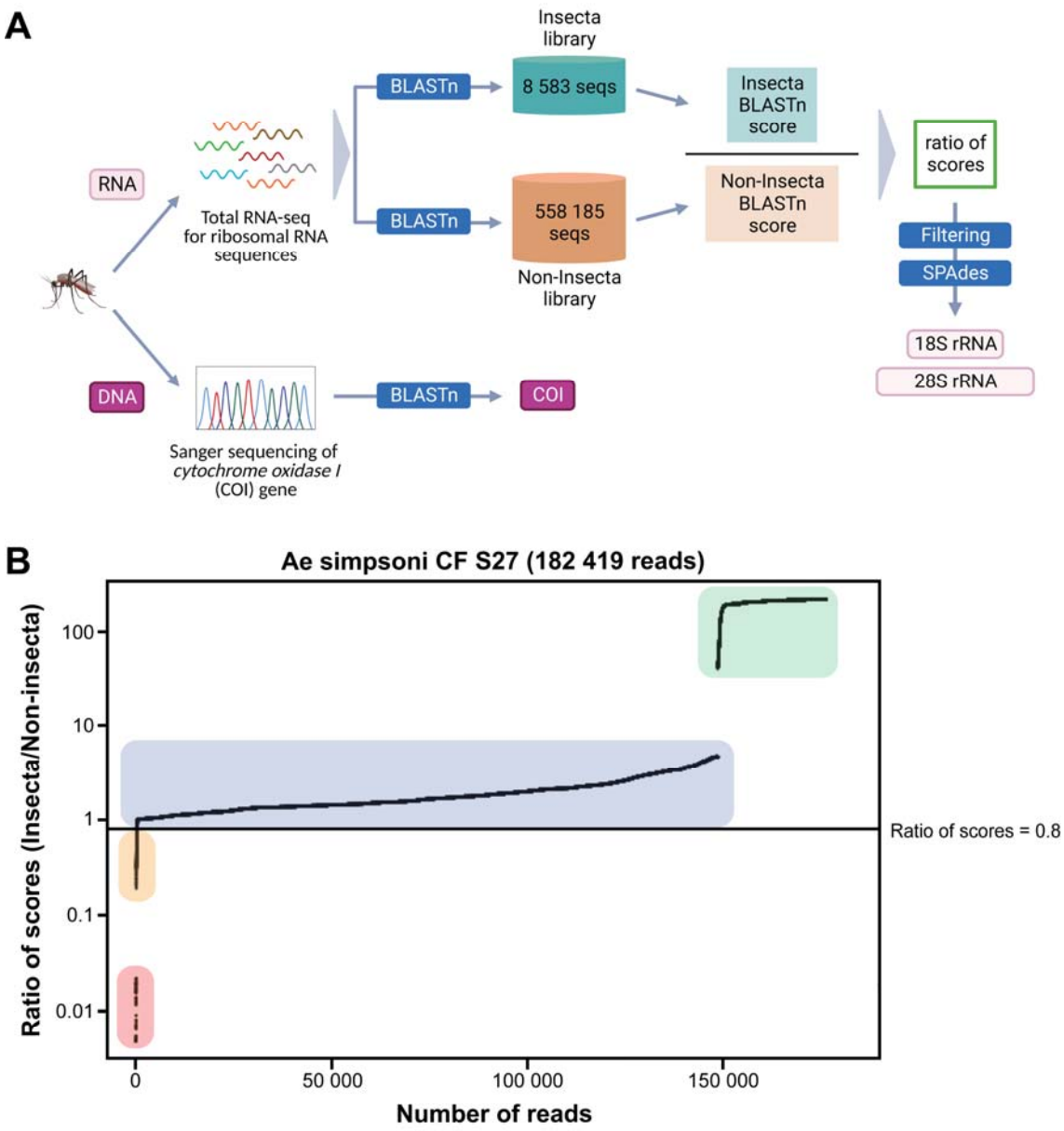

Figure 2. Novel mosquito rRNA sequences were obtained using a unique filtering method. (**A**) Schematic of sequencing and bioinformatics analysis performed in this study to obtain full-length 18S and 28S rRNA sequences as well as COI DNA sequences. Nucleic acids were isolated from mosquito specimens for next generation (for rRNA) or Sanger (for COI) sequencing. Two in-house libraries were created from the SILVA rRNA gene database: Insecta and Non-Insecta, which comprises 8 585 sequences and 558 185 sequences, respectively. Following BLASTn analysis against these two libraries, each RNA-seq read is assigned a ratio of BLASTn scores to describe their relative nucleotide similarity to insect rRNA sequences. Based on these ratios of scores, RNA-seq reads can

then be filtered to remove non-mosquito reads prior to assembly with SPAdes to give full-length 18S and 28S rRNA sequences. Image created with Biorender.com. (**B**) Based on their ratio of scores, reads can be segregated into four categories, as shown on this ratio of scores vs. number of reads plot for the representative specimen “Ae simpsoni CF S27”: (i) reads with hits only in the Insecta library (shaded in green), (ii) reads with a higher score against the Insecta library (shaded in blue), (iii) reads with a higher score against the Non-Insecta library (shaded in yellow), and (iv) reads with no hits in the Insecta library (shaded in red). We applied a conservative threshold at 0.8, indicated by the black horizontal line, where only reads above this threshold are used in the assembly with SPAdes. For this given specimen, 175 671 reads (96.3% of total reads) passed the ≥0.8 cut-off, 325 reads (0.18% of total reads) had ratios of scores <0.8, while 6 423 reads (3.52%) did not have hits against the Insecta library.

Comparative phylogeny of novel rRNA sequences relative to existing records

To verify the assembly accuracy of our rRNA sequences, we constructed a comprehensive phylogenetic tree from the full-length 28S rRNA sequences generated from our study and included relevant rRNA sequences publicly available from GenBank (Figure 3). We applied a search criterion for GenBank sequences with at least 95% coverage of our sequence lengths (~4000 bp), aiming to represent as many species or genera as possible. Although we rarely found records for the same species included in our study, the resulting tree showed that our 28S sequences generally clustered according to their respective species and subgenera, supported by moderate to good bootstrap support at terminal nodes. Species taxa generally formed monophyletic clades, with the exception of *An. gambiae* and *Cx. quinquefasciatus*. *An. gambiae* 28S rRNA sequences formed a clade with closely related sequences from *An. arabiensis*, *An. merus*, and *An. coluzzii,* suggesting unusually high interspecies homology for Anophelines or other members of subgenus *Cellia* (Figure 3, in purple, subgenus *Cellia*). Meanwhile, *Cx. quinquefasciatus* 28S rRNA sequences formed a taxon paraphyletic to sister species *Cx. pipiens* (Figure 3, in coral, subgenus *Culex*).

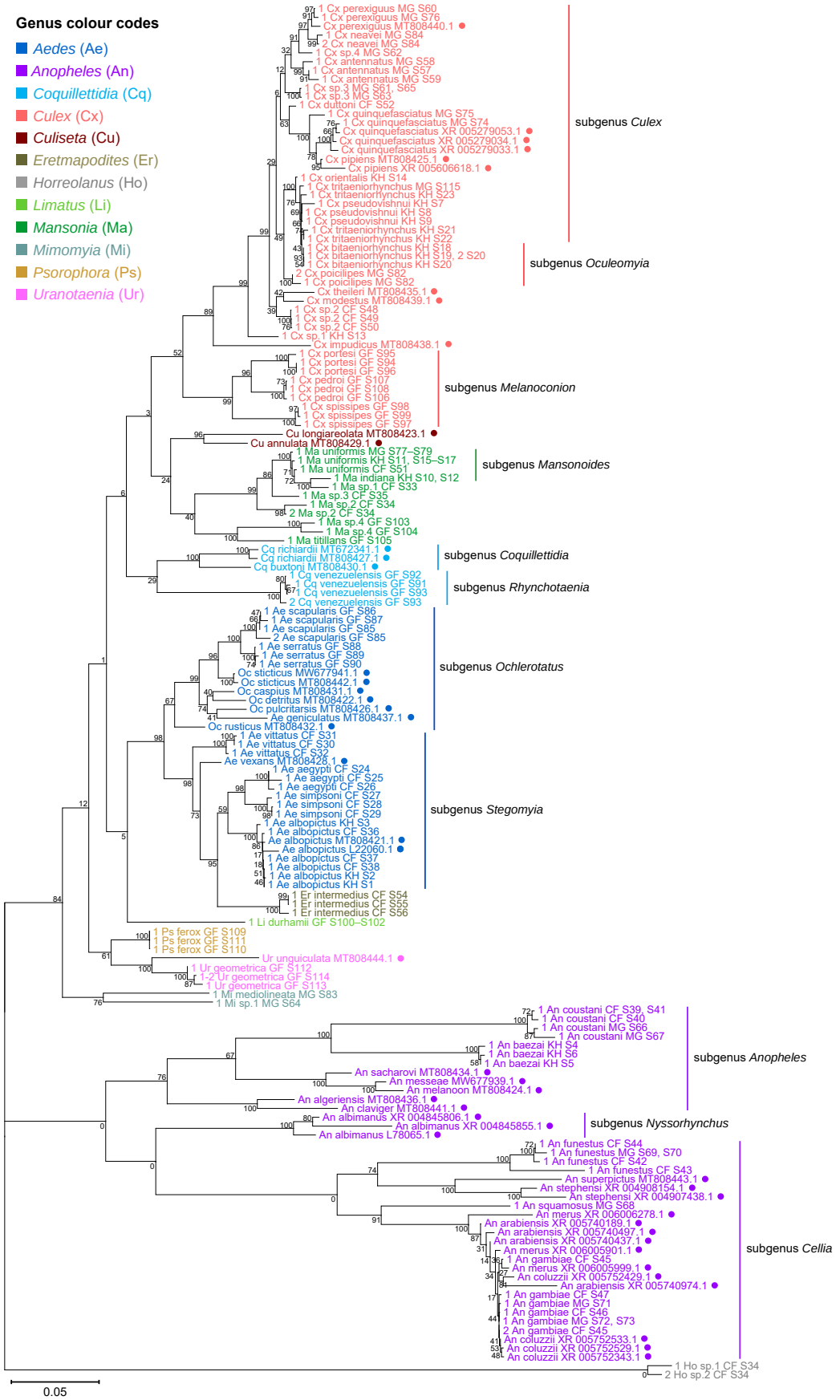
Genus colour codes
Aedes (Ae)
Anopheles (An)
Coquillettidia (Cq)
Culex (Cx)
Culiseta (Cu)
Eretmapodites (Er)
Horreolanus (Ho)
Limatus (Li)
Mansonia (Ma)
Mimomyia (Mi)
Psorophora (Ps)
Uranotaenia (Ur)
subgenus Culex
subgenus Oculeomyia
subgenus Melanoconion
subgenus Mansonoides
subgenus Coquillettidia
subgenus Rhynchotaenia
subgenus Ochlerotatus
subgenus Stegomyia
subgenus Anopheles
subgenus Nyssorhynchus
subgenus Cellia
0.05

Figure 3. 28S sequences generated from this study clustered with conspecifics or congenerics from existing GenBank records. A rooted phylogenetic tree based on full-length 28S sequences (3900 bp) from this study and from GenBank was inferred using the maximum-likelihood method and constructed to scale in MEGA X (S. Kumar et al., 2018) using an unknown *Horreolanus* species found among our samples as an outgroup. Values at each node indicate bootstrap support (%) from 500 replications. Sequences from GenBank are annotated with filled circles and their accession numbers are shown. For sequences from this study, each specimen label contains information on taxonomy, origin (in 2-letter country codes), and specimen ID number. Some specimens produced up to two consensus 28S sequences; this is indicated by the numbers 1 or 2 in the beginning of the specimen label. Specimen genera are indicated by colour: *Culex* in coral, *Anopheles* in purple, *Aedes* in dark blue, *Mansonia* in dark green, *Culiseta* in maroon, *Limatus* in light green, *Coquillettidia* in light blue, *Psorophora* in yellow, *Mimomyia* in teal, *Uranotaenia* in pink and *Eretmapodites* in brown. Scale bar at 0.05 is shown.

28S rRNA sequence-based phylogenetic reconstructions (Figure 3, with GenBank sequences; Figure 4—figure supplement 1, this study only) showed marked incongruence to that of 18S rRNA sequences (Figure 4—figure supplement 2). Although all rRNA trees show the bifurcation of family *Culicidae* into subfamilies *Anophelinae* (genus *Anopheles*, in purple) and *Culicinae* (all other genera), the recovered intergeneric phylogenetic relationships vary between the 28S and 18S rRNA trees and are weakly supported. The 18S rRNA tree also exhibited several taxonomic anomalies: (i) the lack of definitive clustering by species within the *Culex* subgenus (in coral) (ii) the lack of distinction between 18S rRNA sequences of *Cx*. *pseudovishnui* and *Cx*. *Tritaeniorhynchus* (in coral); (iii) the placement of Ma sp. 3 CF S35 (in dark green) within a *Culex* clade; and (iv) the lack of a monophyletic *Mimomyia* clade (in teal) (Figure 4—figure supplement 2). However, 28S and 18S rRNA sequences are encoded by linked loci in rDNA clusters and should not be analysed separately.

Indeed, when concatenated 28S+18S rRNA sequences were generated from the same specimens (Figure 4), the phylogenetic tree resulting from these sequences more closely resembles the 28S tree (Figure 3) with regard to the basal position of the *Mimomyia* clade (in teal) within the *Culicinae* subfamily with good bootstrap support in either tree (84% in 28S rRNA tree, 100% in concatenated 28S+18S rRNA tree). For internal nodes, bootstrap support values were higher in the concatenated tree compared to the 28S tree. Interestingly, the 28S+18S rRNA tree formed an *Aedini* tribe-clade

252 encompassing taxa from genera *Psorophora* (in yellow)*, Aedes* (in dark blue)*,* and *Eretmapodites* (in
253 brown), possibly driven by the inclusion of 18S rRNA sequences. Concatenation also resolved the
254 anomalies found in the 18S rRNA tree and added clarity to the close relationship between *Culex* (in
255 coral) and *Mansonia* (in dark green) taxa. Of note, relative to the 28S tree (Figure 3) the *Culex* and
256 *Mansonia* genera are no longer monophyletic in the concatenated 28S+18S rRNA tree (Figure 4).
257 Genus *Culex* is paraphyletic with respect to subgenus *Mansonoides* of genus *Mansonia* (Figure 3).
258 *Ma*. *titillans* and Ma sp. 4, which we suspect to be *Ma. pseudotitillans,* always formed a distinct branch
259 in 28S or 18S rRNA phylogenies, thus possibly representing a clade of subgenus *Mansonia*.
260 The concatenated 28S+18S rRNA tree (Figure 4) recapitulates what is classically known about the
261 systematics of our specimens, namely (i) the early divergence of subfamily *Anophelinae* from
262 subfamily *Culicinae*, (ii) the division of genus *Anopheles* (in purple) into two subgenera, *Anopheles*
263 and *Cellia,* (iii) the division of genus *Aedes* (in dark blue) into subgenera *Stegomyia* and *Ochlerotatus*,
264 (iv) the divergence of the monophyletic subgenus *Melanoconion* within the *Culex* genus (in coral)
265 (Harbach, 2007; Harbach & Kitching, 2016).

Figure 4. Concatenating 28S and 18S rRNA sequences produces phylogenetic relationships that are concordant with classical *Culicidae* systematics with higher bootstrap support than 28S sequences alone. This phylogenetic tree based on concatenated 28S+18S rRNA sequences (3900+1900 bp) generated from this study was inferred using the maximum-likelihood method and constructed to scale using MEGA X (S. Kumar et al., 2018) using an unknown *Horreolanus* species found among our samples as an outgroup. Values at each node indicate bootstrap support (%) from

500 replications. Each specimen label contains information on taxonomy, origin (as indicated in 2-letter country codes), and specimen ID number. Some specimens produced up to two consensus 28S+18S rRNA sequences; this is indicated by the numbers 1 or 2 in the beginning of the specimen label. Specimen genera are indicated by colour: *Culex* in coral, *Anopheles* in purple, *Aedes* in dark blue, *Mansonia* in dark green, *Limatus* in light green, *Coquillettidia* in light blue, *Psorophora* in yellow, *Mimomyia* in teal, *Uranotaenia* in pink and *Eretmapodites* in brown. Scale bar at 0.05 is shown.

rRNA as a molecular marker for taxonomy and phylogeny

We sequenced a 621 bp region of the COI gene to confirm morphological species identification of our specimens and to compare the functionality of rRNA and COI sequences as molecular markers for taxonomic and phylogenetic investigations. COI sequences were able to unequivocally determine the species identity in most specimens except for the following cases. *An. coustani* COI sequences from our study regardless of specimen origin shared remarkably high nucleotide similarity (>98%) with several other *Anopheles* species such as *An. rhodesiensis*, *An. rufipes*, *An. ziemanni*, *An. tenebrosus*, although *An. coustani* remained the most frequent and closest match. In the case of *Ae. simpsoni*, three specimens had been morphologically identified as *Ae. opok* although their COI sequences showed 97–100% similarity to that of *Ae. simpsoni.* As GenBank held no records of *Ae. opok* COI at the time of this study, we instead aligned the putative *Ae. simpsoni* COI sequences against two sister species of *Ae. opok*: *Ae. luteocephalus* and *Ae. africanus.* We found they shared only 90% and 89% similarity, respectively. Given this significant divergence, we concluded these specimens to be *Ae. simpsoni*. Ambiguous results were especially frequent among *Culex* specimens belonging to the *Cx. pipiens* or *Cx. vishnui* subgroups, where the query sequence differed with either of the top two hits by a single nucleotide. For example, between *Cx. quinquefasciatus* and *Cx. pipiens* of the *Cx. pipiens* subgroup, and between *Cx. vishnui* and *Cx. tritaeniorhynchus* of the *Cx. vishnui* subgroup.

Among our three specimens of *Ma. titillans*, two appeared to belong to a single species that is different from but closely related to *Ma. titillans*. We surmised that these specimens could instead be *Ma. pseudotitillans* based on morphological similarity but were not able to verify this by molecular means as no COI reference sequence is available for this species. These specimens are hence putatively labelled as “Ma sp.4”.

Phylogenetic reconstruction based on the COI sequences showed clustering of all species taxa into distinct clades, underlining the utility of the COI gene in molecular taxonomy (Figure 5)(Hebert et

al., 2003; Ratnasingham & Hebert, 2007). However, species delineation among members of *Culex* subgroups were not as clear cut, although sister species were correctly placed as sister taxa (Figure 5, in coral). This is comparable to the 28S+18S rRNA tree (Figure 4, in coral) and is indicative of lower intraspecies distances relative to interspecies distances.

To evaluate the utility of 28S and 18S rRNA sequences for molecular taxonomy, we used the 28S+18S rRNA tree to discern the identity of six specimens for which COI sequencing could not be performed. These specimens include three unknown *Mansonia* species (Specimen ID S33–S35), a *Ma. uniformis* (Specimen ID S51), an *An. gambiae* (Specimen ID S47), and a *Ur. geometrica* (Specimen ID S113) (Appendix 1—table 1). Their positions in the 28S+18S rRNA tree relative to adjacent taxa confirms the morphological identification of all six specimens to the genus level and, for three of them, to the species level (Figure 4; *Mansonia* in dark green, *Anopheles* in purple, *Uranotaenia* in pink).

The phylogenetic relationships indicated by the COI tree compared to the 28S+18S rRNA tree present only few points of similarity, with key differences summarised in Table 2. COI-based phylogenetic inference indeed showed clustering of generic taxa into monophyletic clades albeit with very weak bootstrap support, except for genera *Culex* and *Mansonia* (Figure 5; *Culex* in coral, *Mansonia* in dark green). Contrary to the 28S+18S rRNA tree (Figure 4), *Culex* subgenus *Melanoconion* was depicted as a polyphyletic taxon with *Cx. spissipes* being a part of the greater *Culicini* clade with members from subgenera *Oculeomyia* and *Culex* while *Cx. pedroi* and *Cx. portesi* formed a distantly related clade. Among the *Mansonia* specimens, the two unknown Ma sp.4 specimens were not positioned as the nearest neighbours of *Ma. titillans* and instead appeared to have diverged earlier from most of the other taxa from the *Culicidae* family. Notably, the COI sequences of genus *Anopheles* (Figure 5, in purple) is not basal to the other members of *Culicidae* and is instead shown to be sister to Culex COI sequences (8% bootstrap support). This is a direct contrast to what is suggested by the rRNA phylogenies (Figures 3 and 4, Figure 4—figure supplements 1 and 2; *Anopheles* in purple), which suggests *Culex* (in coral) rRNA sequences to be among the most recently diverged. Bootstrap support for the more internal nodes of the COI trees were remarkably low compared to those of rRNA-based trees.

In all rRNA trees, it is clear that the interspecific and intersubgeneric evolutionary distances within the genus *Anopheles* are high relative to any other genera, indicating a greater degree of divergence

(Figure 3, Figure 3—figure supplement 1, Figure 4, Figure 4—figure supplements 1 and 2; *Anopheles* in purple). This is evidenced by the longer branch lengths connecting Anopheline species-clades to the node of the most recent common ancestor for subgenera *Anopheles* and *Cellia*. This feature is not evident in the COI tree, where the Anopheline interspecies distances are comparable to those within the *Culex*, *Aedes*, and *Mansonia* taxa (Figure 5; *Anopheles* in purple, *Culex* in coral, *Aedes* in dark blue, *Mansonia* in dark green).

Figure 5. COI sequences cluster by species but show phylogenetic relationships that contrast those derived from rRNA trees. A phylogenetic tree based on COI sequences (621–699 bp) was

inferred using the maximum-likelihood method and constructed to scale using MEGA X (S. Kumar et al., 2018) with three water mite species to serve as outgroups. Outgroup sequences obtained from GenBank are annotated with filled circles and their accession numbers are shown. Values at each node indicate bootstrap support (%) from 500 replications. Each specimen label contains information on taxonomy, origin (as indicated in 2-letter country codes), and specimen ID. Specimen genera are indicted by colour: *Culex* in coral, *Anopheles* in purple, *Aedes* in dark blue, *Mansonia* in dark green, *Limatus* in light green, *Coquillettidia* in light blue, *Psorophora* in yellow, *Mimomyia* in teal, *Uranotaenia* in pink and *Eretmapodites* in brown. Scale bar at 0.05 is shown.

Table 2. Summary of differences between rRNA and COI phylogenies.

Taxa	28S+18S rRNA phylogeny (Figure 4)	COI phylogeny (Figure 5)
The *Anopheles* genus	forms a clade that is basal to the all other members of family *Culicidae*; interspecies branch lengths are notably long	forms a sister clade to the *Culex* genus, and is depicted to have diverged more recently; interspecies branch lengths are comparable to that of other genera
The *Ur. geometrica* species	forms a clade within the *Culicinae* subfamily lineage	forms a clade that is basal to the all other members of family *Culicidae*
The *Aedini* tribe	forms a monophyletic clade comprising the genera *Aedes, Eretmapodites, and Psorophora*, with the latter being an early divergent lineage	does not form a monophyletic clade; the *Psorophora* clade is placed among *Aedes* taxa and the *Eretmapodites* clade is sister to a *Culex* subgenus *Melanoconion* clade
The *Culex* genus	splits into two monophyletic clades with the three French Guyanese species forming a closely-related minor clade	splits into two clades with two out of three French Guyanese species (*Cx. pedroi* and *Cx. portesi*) forming a distantly-related minor clade, while the third (*Cx. spissipes*) is a part of the greater clade
The *Mansonia* genus	is a polyphyletic group comprising two clades with the two French Guyanese taxa forming a distantly-related minor clade; the major clade is placed among *Culex* taxa	forms a subgenus *Mansonoides* clade as per the 28S+18S rRNA tree but the French Guyanese taxa do not cluster together; is depicted to have diverged earlier relative to other taxa in the assemblage
The Ma sp.4 species	forms a sister clade to *Ma. titillans* as part of a minor French Guyanese *Mansonia* clade	does not form a sister clade to *Ma. titillans;* instead is shown to have diverged earlier than all other members of family *Culicidae* after *Ur. geometrica*

On *Culex* subgroups

353 *Culex* (subgenus *Culex*) specimens of this study comprise several closely related sister species
354 belonging to the *Cx. vishnui* and *Cx. univittatus* subgroups, which are notoriously difficult to
355 differentiate based on morphology. Accordingly, in the 28S+18S rRNA (Figure 4, in coral) and COI
356 (Figure 5, in coral) trees these species and their known sister species were clustered together within
357 the *Culex* (subgenus *Culex*) clade: *Cx. tritaeniorhynchus* with *Cx. pseudovishnui* (*Cx. vishnui*
358 subgroup); *Cx. perexiguus* with *Cx. neavei* (*Cx. univittatus* subgroup).
359 The use of the COI sequence to distinguish between members of the *Culex* subgroups was
360 limited. For example, for the two *Cx. quinquefasciatus* samples in our taxonomic assemblage
361 (Specimen ID S74 and S75) (Appendix 1—table 1), BLAST analyses of their COI sequences revealed
362 they are a single nucleotide away from *Cx. pipiens* or *Cx. quinquefasciatus* COI sequences (Appendix
363 2—table 1). In the 28S rRNA tree with GenBank sequences (Figure 3), two *Cx. pipiens* GenBank
364 sequences formed a clade sister to another containing three *Cx. quinquefasciatus* GenBank
365 sequences and the “Cx quinquefasciatus MG S74” sequence with 78% bootstrap support. This is in
366 accordance with other studies examining mitochondrial sequences (Sun et al., 2019) and
367 morphological attributes (Harbach et al., 2017). This shows that the 28S rRNA sequence can
368 distinguish the two species and confirms that “Cx quinquefasciatus MG S74” is indeed a *Cx.*
369 *quinquefasciatus* specimen. However, “Cx quinquefasciatus MG S75” is shown to be basal from other
370 sequences within this *Cx. pipiens* subgroup-clade with 100% bootstrap support. Given that *Cx.*
371 *quinquefasciatus* and *Cx. pipiens* are known to interbreed, it is plausible that this individual is a hybrid
372 of the two species (Farajollahi et al., 2011).

373 **DISCUSSION**

374 RNA-seq metagenomics on field-captured sylvatic mosquitoes is a valuable tool for tracking
375 mosquito viruses through surveillance and virus discovery. However, the lack of reference rRNA
376 sequences hinders good oligo-based depletion and efficient clean-up of RNA-seq data. Additionally,
377 *de novo* assembly of rRNA sequences is complicated due to regions that are highly conserved across
378 all distantly related organisms that could be present in a single specimen, i.e., microbiota, parasites,
379 or vertebrate blood meal. Hence, we sought to establish a method to bioinformatically filter out non-
380 host rRNA reads for the accurate assembly of novel 28S and 18S rRNA reference sequences.

We found that phylogenetic reconstructions based on 28S sequences or concatenated 28S+18S rRNA sequences were able to correctly cluster mosquito taxa according to species and corroborate current mosquito classification. This demonstrates that our bioinformatics methodology reliably generates bona fide 28S and 18S rRNA sequences, even in specimens parasitized by water mites or engorged with vertebrate blood. Further, we were able to use 28S+18S rRNA taxonomy for molecular species identification when COI sequences were unavailable or ambiguous, thus supporting the use of rRNA sequences as a marker. They have the advantage of circumventing the need to additionally isolate and sequence DNA from specimens, as RNA-seq reads can be directly mapped against reference sequences. Post-depletion, in our hands there are sufficient numbers of remaining reads (5–10% of reads per sample) for assembly of complete rRNA contigs (unpublished data).

Phylogenetic inferences based on 28S or 18S rRNA sequences alone do not recover the same interspecific relationships (Figure 4—figure supplements 1 and 2). Relative to 28S sequences, we observed more instances where multiple specimens have near-identical 18S rRNA sequences. This can occur for specimens belonging to the same species, but also for conspecifics sampled from different geographic locations, such as *An. coustani*, *An. gambiae*, or *Ae. albopictus.* More rarely, specimens from the same species subgroup, such as *Cx. pseudovishnui* and *Cx. tritaeniorhynchus*, also shared 18S rRNA sequences. This was surprising given that the 18S rRNA sequences in our dataset is 1900 bp long. Concatenation of 28S and 18S rRNA sequences resolved this issue, enabling species delineation even among sister species of *Culex* subgroups, where morphological identification meets its limits.

In Cambodia and other parts of Asia, the *Cx. vishnui* subgroup includes *Cx*. *tritaeniorhynchus*, *Cx*. *vishnui*, and *Cx*. *pseudovishnui*, which are important vectors of JEV (Maquart & Boyer, 2022). The former two were morphologically identified in our study but later revealed by COI sequencing to be a sister species. Discerning sister species of the *Cx. pipiens* subgroup is further complicated by interspecific breeding, with some populations showing genetic introgression to varying extents (Cornel et al., 2003). The seven sister species of this subgroup are practically indistinguishable based on morphology and require molecular methods to discern (Farajollahi et al., 2011; Zittra et al., 2016). Indeed, the 621 bp COI sequence amplified in our study did not contain enough nucleotide divergence to allow clear identification, given that the COI sequence of *Cx*. *quinquefasciatus* specimens differed from that of *Cx. pipiens* by a single nucleotide. Batovska et al. (2017) found that

411 even the Internal Transcribed Spacer 2 (ITS2) rDNA region, another common molecular marker,
412 could not differentiate the two species. Other DNA molecular markers such as nuclear Ace-2 or CQ11
413 genes (Aspen & Savage, 2003; Zittra et al., 2016) or *Wolbachia pipientis* infection status (Cornel et
414 al., 2003) are typically employed in tandem. In our study, 28S rRNA sequence-based phylogeny
415 validated the identity of specimen “Cx quinquefasciatus MG S74” (Figure 3, in coral) and suggested
416 that specimen “Cx quinquefasciatus MG S75” might have been a *pipiens-quinquefasciatus* hybrid.
417 These examples demonstrate how 28S rRNA sequences, concatenated with 18S rRNA sequences or
418 alone, contain enough resolution to differentiate between *Cx. pipiens* and *Cx*. *quinquefasciatus*.
419 rRNA-based phylogeny thus allows for more accurate species identification and ecological
420 observations in the context of disease transmission. Additionally, tracing the genetic flow across
421 hybrid populations within the *Cx. pipiens* subgroup can inform estimates of vectorial capacity for each
422 species. As only one or two members from the *Cx. pipiens* and *Cx. vishnui* subgroups were
423 represented in our taxonomic assemblage, an explicit investigation including all member species of
424 these subgroups in greater sample numbers is warranted to further test the degree of accuracy with
425 which 28S and 18S rRNA sequences can delineate sister species.
426 Our study included French Guianese *Culex* species *Cx. spissipes* (group Spissipes*)*, *Cx. pedroi*
427 (group Pedroi), and *Cx. portesi* (group Vomerifer). These species belong to the New World subgenus
428 *Melanoconion*, section Spissipes, with well-documented distribution in North and South Americas
429 (Sirivanakarn, 1982) and are vectors of encephalitic alphaviruses EEEV and VEEV among others
430 (Talaga et al., 2021; M. J. Turell et al., 2008; Weaver et al., 2004). Indeed, our rooted rRNA and COI
431 trees showed the divergence of the three *Melanoconion* species from the major *Culex* clade
432 comprising species broadly found across Africa and Asia (Auerswald et al., 2021; Farajollahi et al.,
433 2011; Nchoutpouen et al., 2019; Takhampunya et al., 2011). The topology of the concatenated
434 28S+18S rRNA tree places the *Cx. portesi* and *Cx. pedroi* species-clades as sister groups (92%
435 bootstrap support), with *Cx. spissipes* as a basal group within the *Melanoconion* clade (100%
436 bootstrap support) (Figure 4, in coral). This corroborates the systematics elucidated by Navarro and
437 Weaver (2004) using the ITS2 marker, and those by Sirivanakarn (1982) and Sallum and Forattini
438 (1996) based on morphology. Curiously, in the COI tree, *Cx. Spissipes* sequences were clustered
439 with unknown species Cx. Sp1, forming a clade sister to another containing other *Culex* (*Culex*) and
440 *Culex* (*Oculeomyia*) species, albeit with very low bootstrap support (Figure 5, in coral). Previous

441 phylogenetic studies based on the COI gene have consistently placed *Cx. spissipes* or the Spissipes
442 group basal to other groups within the *Melanoconion* subgenus (Torres-Gutierrez et al., 2016, 2018).
443 However, these studies contain only *Culex* (*Melanoconion*) species in their assemblage, apart from
444 *Cx. quinquefasciatus* to act as an outgroup. This clustering of *Cx. spissipes* with non-*Melanoconion*
445 species in our COI phylogeny could be an artefact of a much more diversified assemblage rather than
446 a true phylogenetic link.

447 Taking advantage of our multi-country sampling, we examined whether rRNA or COI phylogeny
448 can be used to distinguish conspecifics originating from different geographies. Our assemblage
449 contains five of such species: *An. coustani*, *An. funestus*, *An. gambiae*, *Ae. albopictus*, and *Ma.*
450 *uniformis*. Among the rRNA trees, the concatenated 28S+18S and 28S rRNA trees were able to
451 discriminate between *Ma. uniformis* specimens from Madagascar, Cambodia, and the Central African
452 Republic (in dark green), and between *An. coustani* specimens from Madagascar and the Central
453 African Republic (in purple) (100% bootstrap support). In the COI tree, only *Ma. uniformis* was
454 resolved into geographical clades comprising specimens from Madagascar and specimens from
455 Cambodia (in dark green) (72% bootstrap support). No COI sequence was obtained from one *Ma.*
456 *uniformis* specimen from the Central African Republic. The 28S+18S rRNA sequences ostensibly
457 provided more population-level genetic information than COI sequences alone with better support.
458 The use of rRNA sequences in investigating the biodiversity of mosquitoes should therefore be
459 explored with a more comprehensive taxonomic assemblage.

460 The phylogenetic reconstructions based on rRNA or COI sequences in our study are hardly
461 congruent (Table 2), but two principal differences stand out. First, the COI phylogeny does not
462 recapitulate the early divergence of *Anophelinae* from *Culicinae* (Figure 5). This is at odds with other
463 studies estimating mosquito divergence times based on mitochondrial genes (Logue et al., 2013;
464 Lorenz et al., 2021) or nuclear genes (Reidenbach et al., 2009). The second notable feature in the
465 rRNA trees is the remarkably large interspecies and intersubgeneric evolutionary distances within
466 genus *Anopheles* relative to genera in the *Culicinae* subfamily (Figure 3, Figure 3—figure supplement
467 1, Figure 4, Figure 4—figure supplements 1 and 2; *Anopheles* in purple) but this is not apparent in the
468 COI tree. The hyperdiversity among *Anopheles* taxa may be attributed to the earlier diversification of
469 the *Anophelinae* subfamily in the early Cretaceous period compared to that of the *Culicinae* subfamily,
470 a difference of at least 40 million years (Lorenz et al., 2021). The differences in rRNA and COI tree

topologies indicate a limitation in using COI alone to determine evolutionary relationships. Importantly, drawing phylogenetic conclusions from short DNA barcodes such as COI has been cautioned against due to its weak phylogenetic signal (Hajibabaei et al., 2006). The relatively short length of our COI sequences (621–699 bp) combined with the 100-fold higher nuclear substitution rate of mitochondrial genomes relative to nuclear genomes (Arctander, 1995) could result in homoplasy (Danforth et al., 2005), making it difficult to clearly discern ancestral sequences and correctly assign branches into lineages, as evidenced by the poor nodal bootstrap support at genus-level branches. Indeed, in the study by Lorenz et al. (2021), a phylogenetic tree constructed using a concatenation of all 13 protein-coding genes of the mitochondrial genome was able to resolve ancient divergence events. This affirms that while COI sequences can be used to reveal recent speciation events, longer or multi-gene molecular markers are necessary for studies into deeper evolutionary relationships (Danforth et al., 2005).

In contrast to Anophelines where 28S rRNA phylogenies illustrated higher interspecies divergence compared to COI phylogeny, two specimens of an unknown *Mansonia* species, “Ma sp.4 GF S103” and “Ma sp.4 GF S104”, provided an example where interspecies relatedness based on their COI sequences is greater than that based on their rRNA sequences in relation to “Ma titillans GF S105”. While all rRNA trees placed “Ma titillans GF S105” as a sister taxon with 100% bootstrap support, the COI tree placed Ma sp.4 basal to all other species except *Ur. Geometrica* (Figure 5; *Mansonia* in dark green, *Uranotaenia* in pink). This may hint at a historical selective sweep in the mitochondrial genome, whether arising from geographical separation, mutations, or linkage disequilibrium with inherited symbionts (Hurst & Jiggins, 2005), resulting in the disparate mitochondrial haplogroups found in French Guyanese Ma sp.4 and *Ma. titillans*. In addition, both haplogroups are distant from those associated with members of subgenus *Mansonoides*. To note, the COI sequences of “Ma sp.4 GF S103” and “Ma sp.4 GF S104” share 87.12 and 87.39% nucleotide similarity, respectively, to that of “Ma titillans GF S105”. Interestingly, the endosymbiont *Wolbachia pipientis* has been detected in *Ma. titillans* sampled from Brazil (De Oliveira et al., 2015), which may contribute to the divergence of “Ma titillans GF S105” COI sequence away from those of Ma sp.4. This highlights other caveats of using a mitochondrial DNA marker in determining evolutionary relationships (Hurst & Jiggins, 2005), which nuclear markers such as 28S and 18S rRNA sequences may be immune to.

Conclusions

Total RNA-seq is a valuable tool for surveillance and virus discovery in sylvatic mosquitoes but it is impeded by the lack of full-length rRNA reference sequences. Here we presented a rRNA sequence assembly strategy and a dataset of 234 newly generated mosquito 28S and 18S rRNA sequences. Our work has expanded the current mosquito rRNA reference library by providing, to our knowledge, the first full-length rRNA records for 30 species in public databases and paves the way for the assembly of many more. These novel rRNA sequences can improve mosquito metagenomics based on RNA-seq by enabling physical and computational removal of rRNA from specimens and streamlined species identification using rRNA markers.

Given that a reference sequence is available, rRNA markers could serve as a better approach for mosquito taxonomy and phylogeny than COI markers. In analysing the same set of specimens by their COI and rRNA sequences, we showed that rRNA sequences can discriminate between members of a species subgroup as well as conspecifics from different geographies. Phylogenetic inferences from a tree based on 28S rRNA sequences alone or on concatenated 28S+18S rRNA sequences are more aligned with contemporary mosquito systematics, showing evolutionary relationships that agree with other phylogenetic studies. While COI-based phylogeny can reveal recent speciation events, rRNA sequences may be better suited for investigations of deeper evolutionary relationships as they are less prone to selective sweeps and homoplasy. The advantages and disadvantages of rRNA and COI sequences as molecular markers are summarised in Table 3. Further studies are necessary to reveal how rRNA sequences compare against other nuclear or mitochondrial DNA marker systems (Batovska et al., 2017; Beebe, 2018; Behura, 2006; Ratnasingham & Hebert, 2007; Reidenbach et al., 2009; Vezenegho et al., 2022).

Table 3. Comparison of 28S or concatenated 28S+18S rRNA and COI sequences as molecular markers.

28S+18S rRNA	
Advantages	**Disadvantages**
In RNA-seq metagenomics studies, molecular taxonomy of specimens based on rRNA sequences can be done from RNA-seq data without additional sample preparation or sequencing. 28S rRNA and concatenated 28S+18S rRNA sequences can resolve the identity of specimens where COI sequences were ambiguous, particularly between members of species subgroups.	RNA-seq costs more than Sanger sequencing. Reference rRNA sequences are currently much more limited in breadth compared to other established molecular markers.

28S rRNA and concatenated 28S+18S rRNA sequences can distinguish conspecifics from different geographies for certain species. Phylogenetic inferences based on 28S rRNA and concatenated 28S+18S rRNA sequences show relationships that are more concordant to contemporary mosquito systematics elucidated by other studies and may be a more suitable marker to study deep evolutionary relationships. Being longer and nuclear-encoded, 28S or concatenated 28S+18S rRNA sequences are immune to homoplasy or to selective sweeps that may affect genomes of inherited symbionts such as mitochondria.	
COI	
Advantages	**Disadvantages**
With a larger reference database, the COI is a versatile marker for molecular taxonomy. Being a shorter DNA marker, the COI gene is cost-and time-effective to amplify, sequence, and characterise. Universal primer sets to amplify the COI marker have been developed and tested for many diverse species.	All species taxa clustered into distinct clades but with weaker bootstrap support at internal nodes relative to those of the 28S+18S rRNA tree. For *An. coustani*, and members of *Culex* species subgroups such as *Cx. quinquefasciatus* and *Cx. tritaeniorhynchus*, COI is unable to unequivocally confirm species identity as species can differ by just one nucleotide. Other molecular markers are often used in tandem.

MATERIALS AND METHODS

Sample collection

Mosquito specimens were sampled from 2019 to 2020 by medical entomology teams from the Institut Pasteur de Bangui (Central African Republic, Africa; CF), Institut Pasteur de Madagascar (Madagascar, Africa; MG), Institut Pasteur du Cambodge (Cambodia, Asia; KH), and Institut Pasteur de la Guyane (French Guiana, South America; GF). Adult mosquitoes were sampled using several techniques including CDC light traps, BG sentinels, and human-landing catches. Sampling sites are sylvatic locations including rural settlements in the Central African Republic, Madagascar, and French Guiana and national parks in Cambodia. Mosquitoes were morphologically identified using taxonomic identification keys (Edwards, 1941; Grjebine, 1966; Huang & Ward, 1981; Oo et al., 2006; Rattanarithikul et al., 2007, 2010; Rattanarithikul, Harbach, et al., 2005; Rattanarithikul, Harrison, et al., 2005; Rattanarithikul, Harrison, Harbach, et al., 2006; Rattanarithikul, Harrison, Panthusiri, et al., 2006; Rueda, 2004) on cold tables before preservation by flash freezing in liquid nitrogen and

transportation in dry ice to Institut Pasteur Paris for analysis. A list of the 112 mosquito specimens included in our taxonomic assemblage and their related information are provided in Appendix 1—table 1. To note, specimen ID S53, S80, and S81 were removed from our assemblage as their species identity could not be determined by COI or rRNA sequencing.

RNA and DNA isolation

Nucleic acids were isolated from mosquito specimens using TRIzol reagent according to manufacturer's protocol (Invitrogen, Thermo Fisher Scientific, Waltham, Massachusetts, USA). Single mosquitoes were homogenised into 200 µL of TRIzol reagent and other of the reagents within the protocol were volume-adjusted accordingly. Following phase separation, RNA were isolated from the aqueous phase while DNA were isolated from the remaining interphase and phenol-chloroform phase. From here, RNA is used to prepare cDNA libraries for next generation sequencing while DNA is used in PCR amplification and Sanger sequencing of the mitochondrial *cytochrome* c *oxidase subunit I* (COI) gene as further described below.

Probe depletion of rRNA

We tested a selective rRNA depletion protocol by Morlan *et al.* (2012) on several mosquito species from the *Aedes*, *Culex*, and *Anopheles* genera. We designed 77 tiled 80 bp DNA probes antisense to the *Ae. aegypti* 28S, 18S, and 5.8S rRNA sequences. A pool of probes at a concentration of 0.04 µM were prepared. To bind probes to rRNA, 1 µL of probes and 2 µL of Hybridisation Buffer (100 mM Tris-HCl and 200 mM NaCl) was added to rRNA samples to a final volume of 20 µL and subjected to a slow-cool incubation starting at 95 ºC for 2 minutes, then cooling to 22 ºC at a rate of 0.1 ºC per second, ending with an additional 5 minutes at 22 ºC. The resulting RNA:DNA hybrids were treated with 2.5 µL Hybridase™ Thermostable RNase H (Epicentre, Illumina, Madison, Wisconsin, USA) and incubated at 37 ºC for 30 minutes. To remove DNA probes, the mix was treated with 1 µL DNase I (Invitrogen) and purified with Agencourt RNAClean XP Beads (Beckman Coulter, Brea, California, USA). The resulting RNA is used for total RNA sequencing to check depletion efficiency.

Total RNA sequencing

To obtain rRNA sequences, RNA samples were quantified on a Qubit Fluorometer (Invitrogen) using the Qubit RNA BR Assay kit (Invitrogen) for concentration adjustment. Non-depleted total RNA was used for library preparation for next generation sequencing using the NEBNext Ultra II RNA Library

Preparation Kit for Illumina (New England Biolabs, Ipswich, Massachusetts, USA) and the NEBNext Multiplex Oligos for Illumina (Dual Index Primers Set 1) (New England Biolabs). Sequencing was performed on a NextSeq500 sequencing system (Illumina, San Diego, California, USA). Quality control of fastq data and trimming of adapters were performed with FastQC and cutadapt, respectively.

28S and 18S rRNA assembly

To obtain 28S and 18S rRNA contigs, we had to first clean our fastq library by separating the reads representing mosquito rRNA from all other reads. To achieve this, we used the SILVA RNA sequence database to create 2 libraries: one containing all rRNA sequences recorded under the "Insecta" node of the taxonomic tree, the other containing the rRNA sequences of many others nodes distributed throughout the taxonomic tree, hence named “Non-Insecta” (Quast et al., 2013). Each read was aligned using the nucleotide Basic Local Alignment Search Tool (BLASTn, **https://blast.ncbi.nlm.nih.gov/**) of the National Center for Biotechnology Information (NCBI) against each of the two libraries and the scores of the best high-scoring segment pairs from the two BLASTns are subsequently used to calculate a ratio of Insecta over Non-Insecta scores (Altschul et al., 1990). Only reads with a ratio greater than 0.8 were used in the assembly. The two libraries being non-exhaustive, we chose this threshold of 0.8 to eliminate only reads that were clearly of a non-insect origin. Selected reads were assembled with the SPAdes genome assembler using the “-rna” option, allowing more heterogeneous coverage of contigs and kmer lengths of 31 , 51 and 71 bases (Bankevich et al., 2012). This method successfully assembled rRNA sequences for all specimens, including a parasitic *Horreolanus* water mite (122 sequences for 28S and 114 sequences for 18S).

Initially, our filtration technique had two weaknesses. First, there is a relatively small number of complete rRNA sequences in the Insecta library from SILVA. To compensate for this, we carried out several filtration cycles, each time adding in the complete sequences produced in previous cycles to the Insecta library. Second, when our mosquito specimens were parasitized by other insects, it was not possible to bioinformatically filter out rRNA reads belonging to the parasite. For these rare cases, we used the " --trusted-contigs" option of the SPAdes assembler (Bankevich et al., 2012), giving it access to the 28S and 18S rRNA sequences of the mosquito closest in terms of taxonomic distance. By doing this, the assembler was able to reconstruct the rRNA of the mosquito as well as the rRNA of the parasitizing insect. All assembled rRNA sequences from this study have been deposited in

GenBank with accession numbers OM350214–OM350327 for 18S rRNA sequences and OM542339–OM542460 for 28S rRNA sequences.

COI amplicon sequencing

The mitochondrial COI gene was amplified from DNA samples using the universal "Folmer" primer set LCO1490 (5'- GGTCAACAAATCATAAAGATATTGG -3') and HCO2198 (5'-TAAACTTCAGGGTGACCAAAAAATCA-3'), as per standard COI marker sequencing practices, producing a 658 bp product (Folmer et al., 1994). PCRs were performed using Phusion High-Fidelity DNA Polymerase (Thermo Fisher Scientific). Every 50 µL reaction contained 10 µL of 5X High Fidelity buffer, 1 µL of 10 mM dNTPs, 2.5 µL each of 10 mM forward (LCO1490) and reverse (HCO2198) primer, 28.5 µL of water, 5 µL of DNA sample, and 0.5 µL of 2 U/µL Phusion DNA polymerase. A 3-step cycling incubation protocol was used: 98 ºC for 30 seconds; 35 cycles of 98 ºC for 10 seconds, 60 ºC for 30 seconds, and 72 ºC for 15 seconds; 72 ºC for 5 minutes ending with a 4 ºC hold. PCR products were size-verified using gel electrophoresis and then gel-purified using the QIAquick Gel Extraction Kit (Qiagen, Hilden, Germany). Sanger sequencing of the COI amplicons were performed by Eurofins Genomics, Ebersberg, Germany.

COI sequence analysis

Forward and reverse COI DNA sequences were end-trimmed to remove bases of poor quality (Q score < 30). At the 5' ends, sequences were trimmed at the same positions such that all forward sequences start with 5'- TTTTGG and all reverse sequences start with 5'- GGNTCT. Forward and reverse sequences were aligned using BLAST to produce a 621 bp consensus sequence. In cases where good quality sequences extends beyond 621 bp, forward and reverse sequences were assembled using Pearl (**https://www.gear-genomics.com/pearl/**) and manually checked for errors against trace files (Rausch et al., 2019, 2020). We successfully assembled a total of 106 COI sequences. All assembled COI sequences from this study have been deposited in GenBank with accession numbers OM630610–OM630715.

COI validation of morphology-based species identification

We analysed assembled COI sequences with BLASTn against the nucleotide collection (nr/nt) database to confirm morphology-based species identification. BLAST analyses revealed 32 cases where top hits indicated a different species identity, taking <95% nucleotide sequence similarity as the

threshold to delineate distinct species (Appendix 2—table 1). In these cases, the COI sequence of the specimen was then BLAST-aligned against a GenBank record representing the morphological species to verify that the revised identity is a closer match by a significant margin, i.e., more than 2% nucleotide sequence similarity. All species names reported hereafter reflect identities determined by COI sequence except for cases where COI-based identities were ambiguous, in which case morphology-based identities were retained. In cases where matches were found within a single genus but of multiple species, specimens were indicated as an unknown member of their genus (e.g., *Culex* sp.). Information of the highest-scoring references for all specimens, including details of ambiguous BLASTn results, are recorded in Appendix 2—table 1.

Within our COI sequences, we found six unidentified *Culex* species (including two that matched to GenBank entries identified only to the genus level), four unidentified *Mansonia* species, and one unidentified *Mimomyia* species. For *An. baezai*, no existing GenBank records were found at the time this analysis was performed.

Phylogenetic analysis

Multiple sequence alignment (MSA) were performed on assembled COI and rRNA sequences using the MUSCLE software (Edgar, 2004; Madeira et al., 2019). As shown in Figure 3—figure supplement 2, the 28S rRNA sequences contain many blocks of highly conserved nucleotides, which makes the result of multiple alignment particularly obvious. We therefore did not test other alignment programs. The multiple alignment of the COI amplicons is even more evident since no gaps are necessary for this alignment.

Phylogenetic tree reconstructions were performed with the MEGA X software using the maximum-likelihood method (S. Kumar et al., 2018). Default parameters were used with bootstrapping with 500 replications to quantify confidence level in branches. For rRNA trees, sequences belonging to an unknown species of parasitic water mite (genus *Horreolanus*) found in our specimens served as an outgroup taxon. In addition, we created and analysed a separate dataset combining our 28S rRNA sequences and full-length 28S rRNA sequences from GenBank totalling 169 sequences from 58 species (12 subgenera). To serve as outgroups for the COI tree, we included sequences obtained from GenBank of three water mite species, *Horreolanus orphanus* (KM101004), *Sperchon fuxiensis* (MH916807), and *Arrenurus* sp. (MN362807).

DECLARATIONS

Availability of data and materials

The multiple sequence alignments that gave rise to the presented phylogenetic reconstructions are included as source data files linked to the relevant figures. All sequences generated in this study have been deposited in GenBank under the accession numbers OM350214–OM350327 for 18S rRNA sequences, OM542339–OM542460 for 28S rRNA sequences, and OM630610–OM630715 for COI sequences (Appendix 1—table 1).

Competing interests

The authors declare that they have no financial or non-financial competing interests.

Impact statement

A score-based read filtration strategy enables assembly of full-length ribosomal RNA sequences for lesser-studied mosquito species, opening the doors to the use of these sequences as a novel molecular marker for taxonomic and phylogenetic studies.

Funding

This work was supported by the Defence Advanced Research Projects Agency PREEMPT program managed by Dr. Rohit Chitale and Dr. Kerri Dugan [Cooperative Agreement HR001118S0017] (the content of the information does not necessarily reflect the position or the policy of the U.S. government, and no official endorsement should be inferred).

Acknowledgements

We thank members of the Saleh lab for valuable discussions and to Dr Louis Lambrechts for critical reading of the manuscript. We especially thank all medical entomology staff of IP Bangui, IP Cambodge (Sony Yean, Kimly Heng, Kalyan Chhuoy, Sreynik Nhek, Moeun Chhum, Kimhuor Sour and Pierre-Olivier Maquart), IP Madagascar, and IP Guyane for assistance in field missions, laboratory work, and logistics, and Inès Partouche from IP Paris for laboratory assistance. We are also grateful to Dr Catherine Dauga for advice on phylogenetic analyses, and to Amandine Guidez for providing a French Guiana-specific COI reference library. Finally, we thank our reviewers, including Leslie Vosshall and Katherine Young, for their constructive reviews of this manuscript.

FIGURE SUPPLEMENTS

Figure 3—figure supplement 1

Interspecific and intersubgeneric distances within the genus *Anopheles* indicate a greater degree of divergence than those within any other genera of family *Culicidae*. The phylogenetic tree presented in Figure 3 based on 28S sequences from this study and from GenBank (annotated with filled circles) is depicted here in radial format to illustrate how the branch lengths separating Anopheline taxa are longer relative to other members of family *Culicidae*. An unknown Horreolanus

690 species found among our samples serves as an outgroup. For sequences from this study, each
691 specimen label contains information on taxonomy, origin (in 2-letter country codes), and specimen ID
692 number. Specimen genera are indicated by colour: *Culex* in coral, *Anopheles* in purple, *Aedes* in dark
693 blue, *Mansonia* in dark green, *Limatus* in light green, *Coquillettidia* in light blue, *Psorophora* in yellow,
694 *Mimomyia* in teal, *Uranotaenia* in pink and *Eretmapodites* in brown. Scale bar at 0.05 is shown.

695 **Figure 3—figure supplement 2**

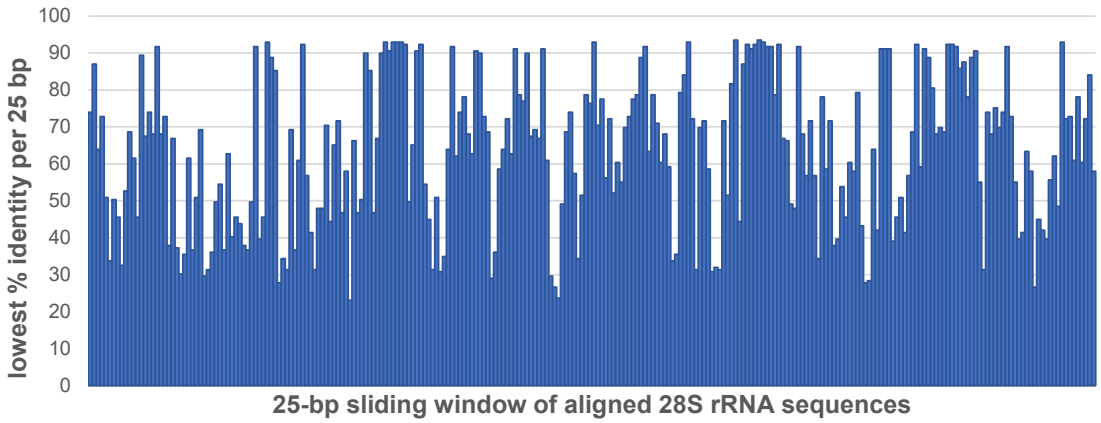

696

697 **Sequence conservation among 169 28S rRNA sequences obtained from this study and from**
698 **GenBank combined**. Multiple sequence alignment was performed on 28S rRNA sequences, 3900 bp
699 in length. Each bar represents a 25-bp sliding window of the 28S rRNA sequence alignment where
700 the y-axis values are the lowest percentage nucleotide identity found.

701 **Figure 4—figure supplement 1**

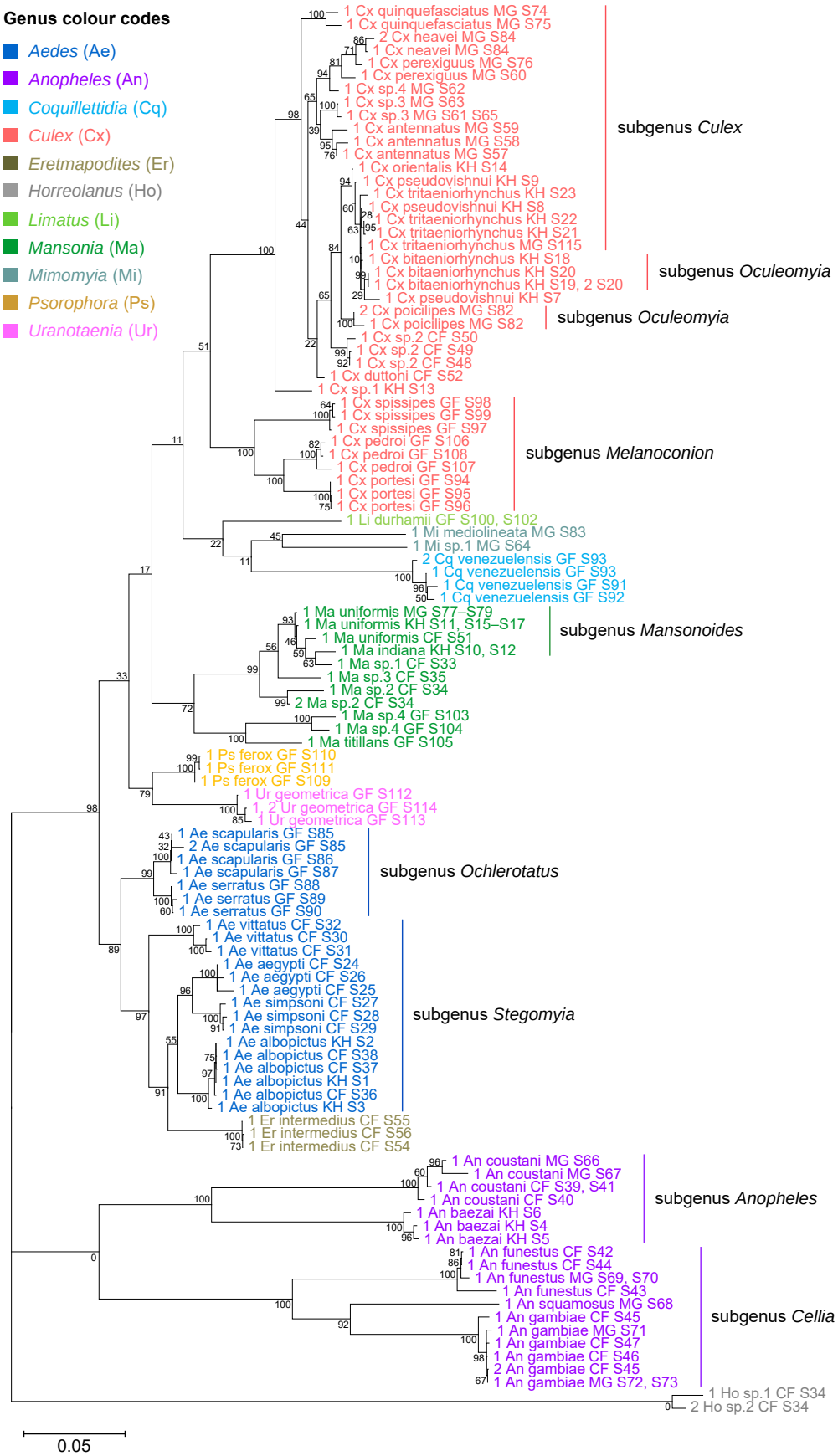
Genus colour codes
Aedes (Ae)
Anopheles (An)
Coquillettidia (Cq)
Culex (Cx)
Eretmapodites (Er)
Horreolanus (Ho)
Limatus (Li)
Mansonia (Ma)
Mimomyia (Mi)
Psorophora (Ps)
Uranotaenia (Ur)
1 Cx quinquefasciatus MG S74
1 Cx quinquefasciatus MG S75
2 Cx neavei MG S84
1 Cx neavei MG S84
1 Cx perexiguus MG S76
1 Cx perexiguus MG S60
1 Cx sp.4 MG S62
1 Cx sp.3 MG S63
1 Cx sp.3 MG S61 S65
1 Cx antennatus MG S59
1 Cx antennatus MG S58
1 Cx antennatus MG S57
subgenus Culex
1 Cx orientalis KH S14
1 Cx pseudovishnui KH S9
1 Cx tritaeniorhynchus KH S23
1 Cx pseudovishnui KH S8
1 Cx tritaeniorhynchus KH S22
1 Cx tritaeniorhynchus KH S21
1 Cx tritaeniorhynchus MG S115
1 Cx bitaeniorhynchus KH S18
1 Cx bitaeniorhynchus KH S20
1 Cx bitaeniorhynchus KH S19, 2 S20
subgenus Oculeomyia
1 Cx pseudovishnui KH S7
2 Cx poicilipes MG S82
1 Cx poicilipes MG S82
subgenus Oculeomyia
1 Cx sp.2 CF S50
1 Cx sp.2 CF S49
1 Cx sp.2 CF S48
1 Cx duttoni CF S52
1 Cx sp.1 KH S13
1 Cx spissipes GF S98
1 Cx spissipes GF S99
1 Cx spissipes GF S97
1 Cx pedroi GF S106
1 Cx pedroi GF S108
1 Cx pedroi GF S107
1 Cx portesi GF S94
1 Cx portesi GF S95
1 Cx portesi GF S96
subgenus Melanoconion
1 Li durhamii GF S100, S102
1 Mi mediolineata MG S83
1 Mi sp.1 MG S64
2 Cq venezuelensis GF S93
1 Cq venezuelensis GF S93
1 Cq venezuelensis GF S91
1 Cq venezuelensis GF S92
1 Ma uniformis MG S77–S79
1 Ma uniformis KH S11, S15–S17
1 Ma uniformis CF S51
1 Ma indiana KH S10, S12
1 Ma sp.1 CF S33
1 Ma sp.3 CF S35
1 Ma sp.2 CF S34
2 Ma sp.2 CF S34
1 Ma sp.4 GF S103
1 Ma sp.4 GF S104
1 Ma titillans GF S105
subgenus Mansonoides
1 Ps ferox GF S110
1 Ps ferox GF S111
1 Ps ferox GF S109
1 Ur geometrica GF S112
1, 2 Ur geometrica GF S114
1 Ur geometrica GF S113
1 Ae scapularis GF S85
2 Ae scapularis GF S85
1 Ae scapularis GF S86
1 Ae scapularis GF S87
1 Ae serratus GF S88
1 Ae serratus GF S89
1 Ae serratus GF S90
subgenus Ochlerotatus
1 Ae vittatus CF S32
1 Ae vittatus CF S30
1 Ae vittatus CF S31
1 Ae aegypti CF S24
1 Ae aegypti CF S26
1 Ae aegypti CF S25
1 Ae simpsoni CF S27
1 Ae simpsoni CF S28
1 Ae simpsoni CF S29
1 Ae albopictus KH S2
1 Ae albopictus CF S38
1 Ae albopictus CF S37
1 Ae albopictus KH S1
1 Ae albopictus CF S36
1 Ae albopictus KH S3
subgenus Stegomyia
1 Er intermedius CF S55
1 Er intermedius CF S56
1 Er intermedius CF S54
1 An coustani MG S66
1 An coustani MG S67
1 An coustani CF S39, S41
1 An coustani CF S40
1 An baezai KH S6
1 An baezai KH S4
1 An baezai KH S5
subgenus Anopheles
1 An funestus CF S42
1 An funestus CF S44
1 An funestus MG S69, S70
1 An funestus CF S43
1 An squamosus MG S68
1 An gambiae CF S45
1 An gambiae MG S71
1 An gambiae CF S47
1 An gambiae CF S46
2 An gambiae CF S45
1 An gambiae MG S72, S73
subgenus Cellia
1 Ho sp.1 CF S34
2 Ho sp.2 CF S34
0.05

702

Phylogenetic tree based on 28S rRNA sequences generated from this study (3900 bp). This tree was inferred using maximum-likelihood method and constructed to scale in MEGA X (S. Kumar et al., 2018) using an unknown *Horreolanus* species found among our samples as an outgroup. Values at each node indicate bootstrap support (%) from 500 replications. For sequences from this study, each specimen label contains information on taxonomy, origin (in 2-letter country codes), and specimen ID number. Some specimens produced up to two consensus 28S rRNA sequences; this is indicated by the numbers 1 or 2 in the beginning of the specimen label. Specimen genera are indicated by colour: *Culex* in coral, *Anopheles* in purple, *Aedes* in dark blue, *Mansonia* in dark green, *Limatus* in light green, *Coquillettidia* in light blue, *Psorophora* in yellow, *Mimomyia* in teal, *Uranotaenia* in pink and *Eretmapodites* in brown. Scale bar at 0.05 is shown.

Figure 4—figure supplement 2

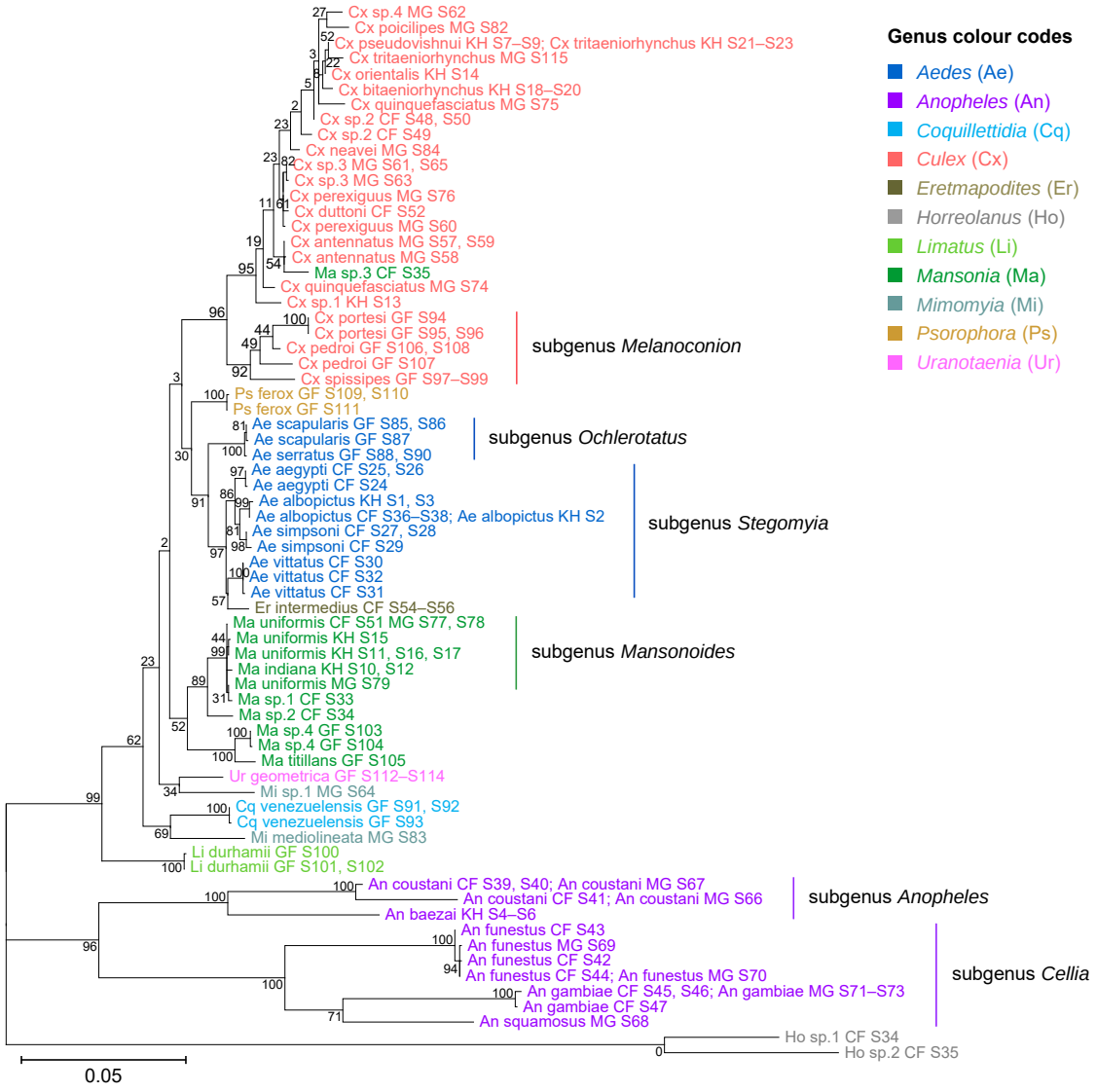

Phylogenetic tree based on 18S rRNA sequences (1900 bp). This tree was inferred using maximum-likelihood method and constructed to scale in MEGA X (S. Kumar et al., 2018) using an unknown *Horreolanus* species found among our samples as an outgroup. Values at each node indicate bootstrap support (%) from 500 replications. For sequences from this study, each specimen label contains information on taxonomy, origin (in 2-letter country codes), and specimen ID number. One 18S rRNA sequence was obtain for each specimen. Specimen genera are indicated by colour: *Culex* in coral, *Anopheles* in purple, *Aedes* in dark blue, *Mansonia* in dark green, *Limatus* in light green, *Coquillettidia* in light blue, *Psorophora* in yellow, *Mimomyia* in teal, *Uranotaenia* in pink and *Eretmapodites* in brown. Scale bar at 0.05 is shown.

APPENDICES

Appendix 1—table 1. Taxonomic and sampling information on mosquito specimens and associated accession numbers of their COI, 18S rRNA, and 28S rRNA sequences (XLSX).

Sequence ID	Taxonomy [Genus (subgenus) species]	Origin	Collection site	Collection period	Blood engorged (Y/N)	Sample ID	COI accession number	18S rRNA accession number	28S rRNA accession number
Ae_albopictus_KH_S1	Aedes (Stegomyia) albopictus	Cambodia	Rattanakiri	Dec 2019	N	1	OM630613	OM350214	OM542460
Ae_albopictus_KH_S2	Aedes (Stegomyia) albopictus	Cambodia	Rattanakiri	Dec 2019	N	2	OM630614	OM350220	OM542373
Ae_albopictus_KH_S3	Aedes (Stegomyia) albopictus	Cambodia	Rattanakiri	Dec 2019	N	3	OM630615	OM350316	OM542374
An_baezai_KH_S4	Anopheles (Anopheles) baezai	Cambodia	Koh Kong	Mar 2019	N	4	OM630631	OM350327	OM542357
An_baezai_KH_S5	Anopheles (Anopheles) baezai	Cambodia	Koh Kong	Mar 2019	N	5	OM630632	OM350233	OM542440
An_baezai_KH_S6	Anopheles (Anopheles) baezai	Cambodia	Koh Kong	Mar 2019	N	6	OM630633	OM350234	OM542358
Cx_pseudovishnui_KH_S7	Culex (Culex) pseudovishnui	Cambodia	Rattanakiri	Dec 2019	N	7	OM630689	OM350285	OM542413
Cx_pseudovishnui_KH_S8	Culex (Culex) pseudovishnui	Cambodia	Rattanakiri	Dec 2019	N	8	OM630690	OM350286	OM542414
Cx_pseudovishnui_KH_S9	Culex (Culex) pseudovishnui	Cambodia	Rattanakiri	Dec 2019	N	9	OM630691	OM350287	OM542415
Ma_indiana_KH_S10	Mansonia (Mansonioides) indiana	Cambodia	Battambong	Nov 2019	N	10	OM630698	OM350295	OM542422
Ma_uniformis_KH_S11	Mansonia (Mansonioides) uniformis	Cambodia	Battambong	Nov 2019	N	11	OM630699	OM350296	OM542423
Ma_indiana_KH_S12	Mansonia	Cambodia	Battambong	Nov 2019	N	12	OM630700	OM350297	OM542424

	(Mansonioides) indiana								
Cx_sp.1_KH_S13	Culex sp.1	Cambodia	Prek Toal	Feb 2019	N	13	OM630672	OM350267	OM542395
Cx_orientalis_KH_S14	Culex (Culex) orientalis	Cambodia	Prek Toal	Feb 2019	N	14	OM630673	OM350268	OM542396
Ma_uniformis_KH_S15	Mansonia (Mansonioides) uniformis	Cambodia	Battambong	Nov 2019	N	15	OM630705	OM350303	OM542430
Ma_uniformis_KH_S16	Mansonia (Mansonioides) uniformis	Cambodia	Battambong	Nov 2019	N	16	OM630706	OM350305	OM542432
Ma_uniformis_KH_S17	Mansonia (Mansonioides) uniformis	Cambodia	Battambong	Nov 2019	N	17	OM630707	OM350304	OM542431
Cx_bitaeniorhynchus_KH_S18	Culex (Oculeomyia) bitaeniorhynchus	Cambodia	Battambong	Nov 2019	N	18	OM630656	OM350255	OM542381
Cx_bitaeniorhynchus_KH_S19	Culex (Oculeomyia) bitaeniorhynchus	Cambodia	Battambong	Nov 2019	N	19	OM630657	OM350256	OM542382
Cx_bitaeniorhynchus_KH_S20	Culex (Oculeomyia) bitaeniorhynchus	Cambodia	Battambong	Nov 2019	N	20	OM630658	OM350257	OM542383, OM542384
Cx_tritaeniorhynchus_KH_S21	Culex (Culex) tritaeniorhynchus	Cambodia	Battambong	Nov 2019	N	21	OM630680	OM350277	OM542404
Cx_tritaeniorhynchus_KH_S22	Culex (Culex) tritaeniorhynchus	Cambodia	Battambong	Nov 2019	N	22	OM630681	OM350278	OM542405
Cx_tritaeniorhynchus_KH_S23	Culex (Culex) tritaeniorhynchus	Cambodia	Battambong	Nov 2019	N	23	OM630682	OM350279	OM542406
Ae_aegypti_CF_S24	Aedes (Stegomyia) aegypti	Central African Republic	Pissa	Jun 2019	N	24	OM630610	OM350314	OM542339
Ae_aegypti_CF_S25	Aedes (Stegomyia) aegypti	Central African Republic	Pissa	Jun 2019	N	25	OM630611	OM350215	OM542340
Ae_aegypti_CF_S26	Aedes (Stegomyia) aegypti	Central African Republic	Pissa	Jun 2019	N	26	OM630612	OM350216	OM542341
Ae_simpsoni_CF_S27	Aedes (Stegomyia) simpsoni	Central African Republic	Pissa	Jun 2019	N	27	OM630619	OM350221	OM542345
Ae_simpsoni_CF_S28	Aedes (Stegomyia)	Central African	Pissa	Jun 2019	N	28	OM630620	OM350222	OM542346

	simpsoni	Republic							
Ae_simpsoni_CF_S29	Aedes (Stegomyia) simpsoni	Central African Republic	Pissa	Jun 2019	N	29	OM630621	OM350223	OM542347
Ae_vittatus_CF_S30	Aedes (Fredwardsius) vittatus	Central African Republic	Gbozo	Aug 2019	Y	30	OM630628	OM350230	OM542439
Ae_vittatus_CF_S31	Aedes (Fredwardsius) vittatus	Central African Republic	Gbozo	Aug 2019	N	31	OM630629	OM350231	OM542355
Ae_vittatus_CF_S32	Aedes (Fredwardsius) vittatus	Central African Republic	Gbozo	Aug 2019	N	32	OM630630	OM350232	OM542356
Ma_sp.1_CF_S33	Mansonia sp.1	Central African Republic	Bayanga	Nov 2019	Y	33	N/A	OM350294	OM542449
Ma_sp.2_CF_S34	Mansonia sp.2	Central African Republic	Bayanga	Nov 2019	Y	34	N/A	OM350322	OM542450, OM542456
Ho_sp.1_CF_S34	Horreolanus sp.1	Central African Republic	Bayanga	Nov 2019	-	34	N/A	OM350325	OM542457
Ho_sp.2_CF_S34	Horreolanus sp.2	Central African Republic	Bayanga	Nov 2019	-	34	N/A	OM350326	OM542458
Ma_sp.3_CF_S35	Mansonia sp.3	Central African Republic	Bayanga	Nov 2019	Y	35	N/A	OM350323	OM542451
Ae_albopictus_CF_S36	Aedes (Stegomyia) albopictus	Central African Republic	Pissa	Jun 2019	N	36	OM630616	OM350217	OM542342
Ae_albopictus_CF_S37	Aedes (Stegomyia) albopictus	Central African Republic	Pissa	Jun 2019	N	37	OM630617	OM350218	OM542343
Ae_albopictus_CF_S38	Aedes (Stegomyia) albopictus	Central African Republic	Pissa	Jun 2019	N	38	OM630618	OM350219	OM542344
An_coustani_CF_S39	Anopheles (Anopheles) coustani	Central African Republic	Pissa	Jan 2020	N	39	OM630634	OM350235	OM542359
An_coustani_CF_S40	Anopheles (Anopheles) coustani	Central African Republic	Pissa	Jan 2020	N	40	OM630635	OM350236	OM542360

An_coustani_CF_S41	Anopheles (Anopheles) coustani	Central African Republic	Pissa	Jan 2020	N	41	OM630636	OM350237	OM542361
An_funestus_CF_S42	Anopheles (Cellia) funestus	Central African Republic	Pissa	Jun 2019	Y	42	OM630640	OM350241	OM542365
An_funestus_CF_S43	Anopheles (Cellia) funestus	Central African Republic	Pissa	Jun 2019	Y	43	OM630641	OM350242	OM542366
An_funestus_CF_S44	Anopheles (Cellia) funestus	Central African Republic	Pissa	Jun 2019	Y	44	OM630642	OM350243	OM542367
An_gambiae_CF_S45	Anopheles (Cellia) gambiae	Central African Republic	Pissa	Jun 2019	Y	45	OM630645	OM350245	OM542369, OM542370
An_gambiae_CF_S46	Anopheles (Cellia) gambiae	Central African Republic	Pissa	Jun 2019	Y	46	OM630646	OM350246	OM542371
An_gambiae_CF_S47	Anopheles (Cellia) gambiae	Central African Republic	Pissa	Jun 2019	Y	47	N/A	OM350247	OM542372
Cx_sp.2_CF_S48	Culex sp.2	Central African Republic	Bayanga	Nov 2019	Y	48	OM630669	OM350269	OM542446
Cx_sp.2_CF_S49	Culex sp.2	Central African Republic	Bayanga	Nov 2019	Y	49	OM630670	OM350315	OM542397
Cx_sp.2_CF_S50	Culex sp.2	Central African Republic	Bayanga	Nov 2019	Y	50	OM630671	OM350270	OM542398
Ma_uniformis_CF_S51	Mansonia (Mansonioides) uniformis	Central African Republic	Bouar	May 2019	Y	51	N/A	OM350301	OM542428
Cx_duttoni_CF_S52	Culex (Culex) duttoni	Central African Republic	Mbaiki	Jan 2019	Y	52	OM630704	OM350302	OM542429
Er_intermedius_CF_S54	Eretmapodites intermedius	Central African Republic	Pissa	Jun 2019	N	54	OM630692	OM350288	OM542416
Er_intermedius_CF_S55	Eretmapodites intermedius	Central African Republic	Pissa	Jun 2019	N	55	OM630693	OM350289	OM542417
Er_intermedius_CF_S56	Eretmapodites	Central	Pissa	Jun 2019	N	56	OM630694	OM350290	OM542418

	intermedius	African Republic							
Cx_antennatus_MG_S57	Culex (Culex) antennatus	Madagascar	Ambato Boeny	Feb 2019	N	57	OM630653	OM350253	OM542379
Cx_antennatus_MG_S58	Culex (Culex) antennatus	Madagascar	Ambato Boeny	Feb 2019	N	58	OM630654	OM350319	OM542444
Cx_antennatus_MG_S59	Culex (Culex) antennatus	Madagascar	Ambato Boeny	Feb 2019	N	59	OM630655	OM350254	OM542380
Cx_perexiguus_MG_S60	Culex (Culex) perexiguus	Madagascar	Amparafaravola	Feb 2019	N	60	OM630660	OM350258	OM542386
Cx_sp.3_MG_S61	Culex sp.3	Madagascar	Ambato Boeny	Aug 2019	N	61	OM630661	OM350259	OM542387
Cx_sp.4_MG_S62	Culex sp.4	Madagascar	Ambato Boeny	Aug 2019	N	62	OM630662	OM350260	OM542388
Cx_sp.3_MG_S63	Culex sp.3	Madagascar	Ambato Boeny	Feb 2019	N	63	OM630686	OM350282	OM542410
Mi_sp.1_MG_S64	Mimomyia sp.1	Madagascar	Ambato Boeny	Feb 2019	N	64	OM630687	OM350283	OM542411
Cx_sp.3_MG_S65	Culex sp.3	Madagascar	Ambato Boeny	Feb 2019	N	65	OM630688	OM350284	OM542412
An_coustani_MG_S66	Anopheles (Anopheles) coustani	Madagascar	Ambato Boeny	Feb 2019	N	66	OM630637	OM350238	OM542362
An_coustani_MG_S67	Anopheles (Anopheles) coustani	Madagascar	Ambato Boeny	Feb 2019	N	67	OM630638	OM350239	OM542363
An_squamosus_MG_S68	Anopheles (Cellia) squamosus	Madagascar	Ambato Boeny	Feb 2019	N	68	OM630639	OM350240	OM542364
An_funestus_MG_S69	Anopheles (Cellia) funestus	Madagascar	Ambato Boeny	Feb 2019	N	69	OM630643	OM350244	OM542368
An_funestus_MG_S70	Anopheles (Cellia) funestus	Madagascar	Ambato Boeny	Feb 2020	N	70	OM630644	OM350317	OM542441
An_gambiae_MG_S71	Anopheles (Cellia) gambiae	Madagascar	Ambato Boeny	Feb 2019	N	71	OM630647	OM350249	OM542442
An_gambiae_MG_S72	Anopheles (Cellia) gambiae	Madagascar	Ambato Boeny	Feb 2019	N	72	OM630648	OM350248	OM542443
An_gambiae_MG_S73	Anopheles (Cellia) gambiae	Madagascar	Ambato Boeny	Feb 2019	N	73	OM630649	OM350318	OM542459
Cx_quinquefasciatus_MG_S74	Culex (Culex) quinquefasciatus	Madagascar	Amparafaravola	Feb 2019	N	74	OM630674	OM350271	OM542399
Cx_quinquefasciatus_MG_S75	Culex (Culex) quinquefasciatus	Madagascar	Amparafaravola	Feb 2019	N	75	OM630675	OM350272	OM542447
Cx_perexiguus_MG_S76	Culex (Culex) perexiguus	Madagascar	Mampikony	Aug 2019	N	76	OM630676	OM350273	OM542400

Ma_uniformis_MG_S77	Mansonia (Mansonioides) uniformis	Madagascar	Ambato Boeny	Feb 2019	N	77	OM630708	OM350306	OM542433
Ma_uniformis_MG_S78	Mansonia (Mansonioides) uniformis	Madagascar	Ambato Boeny	Feb 2019	N	78	OM630709	OM350307	OM542434
Ma_uniformis_MG_S79	Mansonia (Mansonioides) uniformis	Madagascar	Ambato Boeny	Feb 2019	N	79	OM630710	OM350308	OM542435
Cx_poicilipes_MG_S82	Culex poicilipes	Madagascar	Mampikony	Feb 2019	N	82	OM630659	OM350320	OM542385, OM542445
Mi_mediolineata_MG_S83	Mimomyia mediolineata	Madagascar	Ambato Boeny	Feb 2019	N	83	OM630683	OM350280	OM542407
Cx_neavei_MG_S84	Culex (Culex) neavei	Madagascar	Ambato Boeny	Feb 2019	N	84	OM630684	OM350281	OM542408, OM542409
Ae_scapularis_GF_S85	Aedes (Ochlerotatus) scapularis	French Guiana	Hameau Prefontaine	Jul 2019	N	85	OM630624	OM350224	OM542348, OM542349
Ae_scapularis_GF_S86	Aedes (Ochlerotatus) scapularis	French Guiana	Hameau Prefontaine	Jul 2019	N	86	OM630622	OM350225	OM542350
Ae_scapularis_GF_S87	Aedes (Ochlerotatus) scapularis	French Guiana	Hameau Prefontaine	Jul 2019	N	87	OM630623	OM350226	OM542351
Ae_serratus_GF_S88	Aedes (Ochlerotatus) serratus	French Guiana	Hameau Prefontaine	Nov 2020	N	88	OM630625	OM350227	OM542352
Ae_serratus_GF_S89	Aedes (Ochlerotatus) serratus	French Guiana	Hameau Prefontaine	Nov 2020	N	89	OM630626	OM350228	OM542353
Ae_serratus_GF_S90	Aedes (Ochlerotatus) serratus	French Guiana	Hameau Prefontaine	Nov 2020	N	90	OM630627	OM350229	OM542354
Cq_venezuelensis_GF_S91	Coquillettidia venezuelensis	French Guiana	Hameau Prefontaine	Jul 2019	N	91	OM630650	OM350250	OM542375
Cq_venezuelensis_GF_S92	Coquillettidia venezuelensis	French Guiana	Hameau Prefontaine	Jul 2019	N	92	OM630651	OM350251	OM542376
Cq_venezuelensis_GF_S93	Coquillettidia venezuelensis	French Guiana	Hameau Prefontaine	Jul 2019	N	93	OM630652	OM350252	OM542377, OM542378
Cx_portesi_GF_S94	Culex sp. BTLHVDV-2014	French Guiana	Hameau Prefontaine	Jul 2019	N	94	OM630666	OM350264	OM542392
Cx_portesi_GF_S95	Culex sp. BTLHVDV-2014	French Guiana	Hameau Prefontaine	Jul 2019	N	95	OM630667	OM350265	OM542393

Cx_portesi_GF_S96	Culex sp. BTLHVDV-2014	French Guiana	Hameau Prefontaine	Jul 2019	N	96	OM630668	OM350266	OM542394
Cx_spissipes_GF_S97	Culex (Melanoconion) sp. DJS-2020	French Guiana	Hameau Prefontaine	Jul 2019	N	97	OM630677	OM350274	OM542401
Cx_spissipes_GF_S98	Culex (Melanoconion) sp. DJS-2020	French Guiana	Hameau Prefontaine	Jul 2019	N	98	OM630678	OM350275	OM542402
Cx_spissipes_GF_S99	Culex (Melanoconion) sp. DJS-2020	French Guiana	Hameau Prefontaine	Jul 2019	N	99	OM630679	OM350276	OM542403
Li_durhamii_GF_S100	Limatus durhamii	French Guiana	Hameau Prefontaine	Jul 2019	N	100	OM630695	OM350291	OM542419
Li_durhamii_GF_S101	Limatus durhamii	French Guiana	Hameau Prefontaine	Jul 2019	N	101	OM630696	OM350292	OM542420
Li_durhamii_GF_S102	Limatus durhamii	French Guiana	Hameau Prefontaine	Jul 2019	N	102	OM630697	OM350293	OM542421
Ma_sp.4_GF_S103	Mansonia sp.4	French Guiana	Hameau Prefontaine	Jan 2020	N	103	OM630701	OM350298	OM542425
Ma_sp.4_GF_S104	Mansonia sp.4	French Guiana	Hameau Prefontaine	Jan 2020	N	104	OM630702	OM350299	OM542426
Ma_titillans_GF_S105	Mansonia (Mansonia) titillans	French Guiana	Hameau Prefontaine	Jan 2020	N	105	OM630703	OM350300	OM542427
Cx_pedroi_GF_S106	Culex (Melanoconion) pedroi	French Guiana	Hameau Prefontaine	Nov 2020	N	106	OM630663	OM350261	OM542389
Cx_pedroi_GF_S107	Culex (Melanoconion) pedroi	French Guiana	Hameau Prefontaine	Nov 2020	N	107	OM630664	OM350262	OM542390
Cx_pedroi_GF_S108	Culex (Melanoconion) pedroi	French Guiana	Hameau Prefontaine	Nov 2020	N	108	OM630665	OM350263	OM542391
Ps_ferox_GF_S109	Psorophora ferox	French Guiana	Iracoubo	2009	N	109	OM630711	OM350309	OM542436
Ps_ferox_GF_S110	Psorophora ferox	French Guiana	Iracoubo	2009	N	110	OM630712	OM350310	OM542437
Ps_ferox_GF_S111	Psorophora ferox	French Guiana	Iracoubo	2009	N	111	OM630713	OM350324	OM542452
Ur_geometrica_GF_S112	Uranotaenia (Uranotaenia) geometrica	French Guiana		2010	N	112	OM630714	OM350311	OM542453
Ur_geometrica_GF_S113	Uranotaenia	French		2010	N	113	N/A	OM350312	OM542454

	(Uranotaenia) geometrica	Guiana								
Ur_geometrica_GF_S114	Uranotaenia (Uranotaenia) geometrica	French Guiana		2010	N	114	OM630715	OM350313	OM542438, OM542455
Cx_tritaeniorhynchus_MG_S115	Culex (Culex) tritaeniorhynchus	Madagascar	Ambato Boeny	Feb 2019	N	115	OM630685	OM350321	OM542448

Appendix 2—table 1. COI sequence BLAST analyses summary (XLSX).

Sequence ID	Sequence length	Morphological identification	BLASTn top hit species	BLASTn top hit accession	Query coverage	E-value	% identity	Comments
Ae_albopictus_KH_S1	699	Aedes albopictus	Aedes albopictus	MK714006.1	99%	0.0	99.71%	
Ae_albopictus_KH_S2	695	Aedes albopictus	Aedes albopictus	MK714006.1	100%	0.0	99.71%	
Ae_albopictus_KH_S3	695	Aedes albopictus	Aedes albopictus	MK714006.1	100%	0.0	99.71%	
An_baezai_KH_S4	658	Anopheles baezai	Anopheles darlingi	MF381626.1	100%	0.0	92.71%	An baezai not found in GenBank databases
An_baezai_KH_S5	670	Anopheles baezai	Anopheles darlingi	MF381626.1	99%	0.0	92.81%	An baezai not found in GenBank databases
An_baezai_KH_S6	659	Anopheles baezai	Anopheles darlingi	MF381626.1	100%	0.0	92.72%	An baezai not found in GenBank databases
Cx_pseudovishnui_KH_S7	660	Culex vishnui	Culex pseudovishnui	MW321882.1	98%	0.0	98.92%	95% similarity to Cx vishnui, 94% similarity with Cx tritaeniorhynchus
Cx_pseudovishnui_KH_S8	659	Culex vishnui	Culex pseudovishnui	MW321882.1	98%	0.0	99.38%	95% similarity to Cx vishnui, 94% similarity with Cx tritaeniorhynchus
Cx_pseudovishnui_KH_S9	659	Culex vishnui	Culex pseudovishnui	MW321882.1	98%	0.0	98.92%	95% similarity to Cx vishnui, 94% similarity with Cx tritaeniorhynchus
Ma_indiana_KH_S10	660	Mansonia indiana	Mansonia indiana	MK637632.1	98.00%	0.0	99.54%	
Ma_uniformis_KH_S11	686	Mansonia indiana	Mansonia uniformis	MK757484.1	99%	0.0	99.71%	89.99% from Ma indiana MK637632.1
Ma_indiana_KH_S12	693	Mansonia indiana	Mansonia indiana	MK637632.1	97%	0.0	99.41%	
Cx_sp.1_KH_S13	687	Culex quinquefasciatus	Culex (Lophoceraomyia) sp. 5 HY-2020	MW321904.1	98%	0.0	94.39%	90% from Cx quinquefasciatus GU188856.2
Cx_orientalis_KH_S14	662	Culex	Culex orientalis	MW228488.1	97%	0.0	98.29%	

		quinquefasciatus						
Ma_uniformis_KH_S15	658	Mansonia uniformis	Mansonia uniformis	MK757484.1	100.00%	0.0	99.54%	
Ma_uniformis_KH_S16	654	Mansonia uniformis	Mansonia uniformis	MK757484.1	100.00%	0.0	99.39%	
Ma_uniformis_KH_S17	657	Mansonia uniformis	Mansonia uniformis	MK757484.1	99.00%	0.0	99.54%	
Cx_bitaeniorhynchus_KH_S18	658	Culex bitaeniorhynchus	Culex bitaeniorhynchus	HQ398898.1	97.00%	0.0	99.69%	
Cx_bitaeniorhynchus_KH_S19	650	Culex bitaeniorhynchus	Culex bitaeniorhynchus	HQ398898.1	98.00%	0.0	99.84%	
Cx_bitaeniorhynchus_KH_S20	652	Culex bitaeniorhynchus	Culex bitaeniorhynchus	HQ398898.1	98.00%	0.0	99.38%	
Cx_tritaeniorhynchus_KH_S21	695	Culex tritaeniorhynchus	Culex vishnui or Culex tritaeniorhynchus	MH374857.1	100%	0.0	99.57%	99.69% to Cx tritaeniorhynchus MF179213.1
Cx_tritaeniorhynchus_KH_S22	690	Culex tritaeniorhynchus	Culex vishnui or Culex tritaeniorhynchus	MT876103.1	100%	0.0	99.57%	
Cx_tritaeniorhynchus_KH_S23	663	Culex tritaeniorhynchus	Culex tritaeniorhynchus	MT876103.1	99%	0.0	98.79%	
Ae_aegypti_CF_S24	689	Aedes aegypti	Aedes aegypti	MN299016.1	100%	0.0	99.56%	
Ae_aegypti_CF_S25	660	Aedes aegypti	Aedes aegypti	MN299024.1	100.00%	0.0	99.70%	
Ae_aegypti_CF_S26	660	Aedes aegypti	Aedes aegypti	MN299024.1	100.00%	0.0	99.70%	
Ae_simpsoni_CF_S27	644	Aedes opok	Aedes simpsoni	LC473669.1	97.00%	0.0	97.77%	Ae opok not found in GenBank, sequence is 90% and 89% away from Ae luteocephalus and Ae africanus, sister species of Ae opok.
Ae_simpsoni_CF_S28	649	Aedes opok	Aedes simpsoni	MN552302.1	99.00%	0.0	100.00%	Ae opok not found in GenBank, sequence is 90% and 89% away from Ae luteocephalus and Ae africanus, sister species of Ae opok.
Ae_simpsoni_CF_S29	627	Aedes opok	Aedes simpsoni	MN552302.1	98.00%	0.0	98.87%	Ae opok not found in GenBank, sequence is 90% and 89% away from Ae luteocephalus and Ae africanus, sister species of Ae opok.
Ae_vittatus_CF_S30	623	Aedes vittatus	Aedes vittatus	MN552298.1	100.00%	0.0	99.84%	
Ae_vittatus_CF_S31	622	Aedes vittatus	Aedes vittatus	MN552298.1	100.00%	0.0	99.68%	

Ae_vittatus_CF_S32	621	Aedes vittatus	Aedes vittatus	MN552298.1	100.00%	0.0	99.68%	
Ma_sp.1_CF_S33	-	Mansonia africana	-	-	-	-	-	No COI obtained
Ma_sp.2_CF_S34	-	Mansonia africana	-	-	-	-	-	No COI obtained
Ma_sp.3_CF_S35	-	Mansonia africana	-	-	-	-	-	No COI obtained
Ae_albopictus_CF_S36	627	Aedes albopictus	Aedes albopictus	MK995332.1	100.00%	0.0	99.84%	
Ae_albopictus_CF_S37	621	Aedes albopictus	Aedes albopictus	MK995332.1	100.00%	0.0	100.00%	
Ae_albopictus_CF_S38	621	Aedes albopictus	Aedes albopictus	MK995332.1	100.00%	0.0	100.00%	
An_coustani_CF_S39	621	Anopheles coustani	Anopheles coustani	MK585968.1	100.00%	0.0	99.84%	
An_coustani_CF_S40	621	Anopheles coustani	Anopheles coustani	MK585959.1	100.00%	0.0	99.03%	
An_coustani_CF_S41	699	Anopheles coustani	Anopheles coustani	MK585968.1	94.00%	0.0	99.70%	
An_funestus_CF_S42	696	Anopheles funestus	Anopheles funestus	MK300231.1	100.00%	0.0	99.71%	
An_funestus_CF_S43	660	Anopheles funestus	Anopheles funestus	MT375215.1	100.00%	0.0	99.85%	
An_funestus_CF_S44	658	Anopheles funestus	Anopheles funestus	MT375215.1	100.00%	0.0	99.70%	
An_gambiae_CF_S45	660	Anopheles gambiae	Anopheles gambiae	MG930895.1	86.00%	0.0	99.79%	
An_gambiae_CF_S46	659	Anopheles gambiae	Anopheles gambiae	MT375223.1	89.00%	0.0	100.00%	
An_gambiae_CF_S47	-	Anopheles gambiae	-	-	-	-	-	No COI obtained
Cx_sp.2_CF_S48	653	Culex quinquefasciatus	Culex corniger	KM593015.1	100.00%	0.0	94.95%	94% to all other Cx species
Cx_sp.2_CF_S49	660	Culex quinquefasciatus	Culex nigripalpus	KM593058.1	99.00%	0.0	94.65%	94% to all other Cx species
Cx_sp.2_CF_S50	658	Culex quinquefasciatus	Culex bidens	MH931446.1	100.00%	0.0	94.68%	94% to all other Cx species
Ma_uniformis_CF_S51	-	Mansonia uniformis	-	-	-	-	-	No COI obtained
Cx_duttoni_CF_S52	621	Mansonia uniformis	Culex duttoni	LC473629.1	100.00%	0.0	99.68%	
Er_intermedius_CF_S54	620	Eretmapodites sp.	Eretmapodites intermedius	MN552305.1	100.00%	0.0	99.52%	
Er_intermedius_CF_S55	621	Eretmapodites sp.	Eretmapodites intermedius	MN552305.1	100.00%	0.0	99.68%	

Er_intermedius_CF_S56	621	Eretmapodites sp.	Eretmapodites intermedius	MN552305.1	100.00%	0.0	99.68%	
Cx_antennatus_MG_S57	621	Culex antennatus	Culex antennatus	LC473659.1	100.00%	0.0	100.00%	
Cx_antennatus_MG_S58	621	Culex antennatus	Culex antennatus	LC473659.1	100.00%	0.0	100.00%	
Cx_antennatus_MG_S59	621	Culex antennatus	Culex antennatus	LC473659.1	100.00%	0.0	100.00%	
Cx_perexiguus_MG_S60	621	Culex decens	Culex perexiguus	LC473634.1	100.00%	0.0	99.84%	
Cx_sp.3_MG_S61	685	Culex decens	Unknown Culex species	KU380436.1	96.00%	0.0	96.05%	
Cx_sp.4_MG_S62	687	Culex decens	Unknown Culex species	MT993494.1	99.00%	0.0	95.63%	
Cx_sp.3_MG_S63	687	Culex univittatus	Unknown Culex species	KU380436.1	95.00%	0.0	96.50%	
Mi_sp.1_MG_S64	694	Culex univittatus	Mimomyia mimomyiaformis	LC473719.1	94.00%	0.0	92.55%	Unknown Mimomyia species
Cx_sp.3_MG_S65	691	Culex univittatus	Unknown Culex species	KU380436.1	95.00%	0.0	96.66%	
An_coustani_MG_S66	669	Anopheles coustani	Anopheles coustani	NC_050693.1	99.00%	0.0	99.40%	
An_coustani_MG_S67	659	Anopheles coustani	Anopheles coustani	NC_050693.1	99.00%	0.0	99.08%	
An_squamosus_MG_S68	653	Anopheles coustani	Anopheles squamosus	MK776741.1	100.00%	0.0	100.00%	
An_funestus_MG_S69	654	Anopheles funestus	Anopheles funestus	MT375215.1	100.00%	0.0	99.85%	
An_funestus_MG_S70	654	Anopheles funestus	Anopheles funestus	MG742199.1	100.00%	0.0	99.69%	
An_gambiae_MG_S71	654	Anopheles gambiae	Anopheles gambiae	MT375222.1	100.00%	0.0	99.85%	
An_gambiae_MG_S72	654	Anopheles gambiae	Anopheles gambiae	MT375222.1	100.00%	0.0	99.85%	
An_gambiae_MG_S73	622	Anopheles gambiae	Anopheles gambiae	MT375222.1	100.00%	0.0	100.00%	
Cx_quinquefasciatus_MG_S74	654	Culex quinquefasciatus	Culex pipiens	MT199095.1	100.00%	0.0	100.00%	99.85% to Cx quinquefasciatus
Cx_quinquefasciatus_MG_S75	647	Culex quinquefasciatus	Culex quinquefasciatus	MH423504.1	100.00%	0.0	98.15%	Also 98% to Cx pipiens
Cx_perexiguus_MG_S76	621	Culex quinquefasciatus	Culex perexiguus	LC473634.1	100.00%	0.0	99.52%	Same SNPs to Cx pipiens MH374861.1
Ma_uniformis_MG_S77	621	Mansonia uniformis	Mansonia uniformis	KU187165.1	100.00%	0.0	100.00%	

Ma_uniformis_MG_S78	621	Mansonia uniformis	Mansonia uniformis	KU187165.1	100.00%	0.0	100.00%	
Ma_uniformis_MG_S79	626	Mansonia uniformis	Mansonia uniformis	KU187157.1	100.00%	0.0	99.68%	
Cx_poicilipes_MG_S82	689	Culex bitaeniorhynchus	Culex poicilipes	LC473618.1	95.00%	0.0	99.70%	
Mi_mediolineata_MG_S83	694	Culex tritaeniorhynchus	Mimomyia mediolineata	LC473723.1	94.00%	0.0	99.39%	
Cx_neavei_MG_S84	671	Culex tritaeniorhynchus	Culex neavei	LC473635.1	98.00%	0.0	99.85%	
Ae_scapularis_GF_S85	659	Aedes scapularis	Aedes scapularis	MN997484.1	97.00%	0.0	98.76%	
Ae_scapularis_GF_S86	658	Aedes scapularis	Aedes scapularis	MF172265.1	97.00%	0.0	99.38%	
Ae_scapularis_GF_S87	654	Aedes scapularis	Aedes scapularis	MF172265.1	98.00%	0.0	99.22%	
Ae_serratus_GF_S88	660	Aedes serratus	Aedes serratus	MF172269.1	97.00%	0.0	98.91%	
Ae_serratus_GF_S89	660	Aedes serratus	Aedes serratus	MF172268.1	97.00%	0.0	99.22%	
Ae_serratus_GF_S90	654	Aedes serratus	Aedes serratus	MF172268.1	98.00%	0.0	99.07%	
Cq_venezuelensis_GF_S91	658	Coquillettidia venezuelensis	Coquillettidia venezuelensis	MN997703.1	97.00%	0.0	97.98%	
Cq_venezuelensis_GF_S92	621	Coquillettidia venezuelensis	Coquillettidia venezuelensis	MN997703.1	100.00%	0.0	98.07%	
Cq_venezuelensis_GF_S93	621	Coquillettidia venezuelensis	Coquillettidia venezuelensis	MN997703.1	100.00%	0.0	97.75%	
Cx_portesi_GF_S94	653	Culex portesi	Culex portesi	in-house reference library			98.5-100%	reference sequence provided by Amandine Guidez, IP Guyane
Cx_portesi_GF_S95	693	Culex portesi	Culex portesi	in-house reference library			98.5-100%	reference sequence provided by Amandine Guidez, IP Guyane
Cx_portesi_GF_S96	687	Culex portesi	Culex portesi	in-house reference library			98.5-100%	reference sequence provided by Amandine Guidez, IP Guyane
Cx_spissipes_GF_S97	672	Culex spissipes	Culex spissipes	in-house reference library			98.5-100%	reference sequence provided by Amandine Guidez, IP Guyane
Cx_spissipes_GF_S98	663	Culex spissipes	Culex spissipes	in-house reference library			98.5-100%	reference sequence provided by Amandine Guidez, IP Guyane
Cx_spissipes_GF_S99	660	Culex spissipes	Culex spissipes	in-house reference library			98.5-100%	reference sequence provided by Amandine Guidez, IP Guyane
Li_durhamii_GF_S100	653	Limatus durhamii	Limatus durhamii	MF172330.1	98.00%	0.0	99.84%	

Li_durhamii_GF_S101	621	Limatus durhamii	Limatus durhamii	MF172330.1	100.00%	0.0	100.00%	
Li_durhamii_GF_S102	699	Limatus durhamii	Limatus durhamii	MF172330.1	94.00%	0.0	100.00%	
Ma_sp.4_GF_S103	621	Mansonia titillans	Mansonia sp.	MT329066.1	100.00%	0.0	99.84%	87.12% to Ma titillans MN968244.1
Ma_sp.4_GF_S104	695	Mansonia titillans	Mansonia sp.	MT329066.1	95.00%	0.0	99.85%	87.39% to Ma titillans MN968244.1
Ma_titillans_GF_S105	669	Mansonia titillans	Mansonia titillans	MN968244.1	98.00%	0.0	99.70%	
Cx_pedroi_GF_S106	653	Culex pedroi	Culex pedroi	KX779887.1	98.00%	0.0	98.60%	
Cx_pedroi_GF_S107	661	Culex pedroi	Culex pedroi	KX779887.1	97.00%	0.0	98.76%	
Cx_pedroi_GF_S108	621	Culex pedroi	Culex pedroi	KX779887.1	99.00%	0.0	98.87%	
Ps_ferox_GF_S109	633	Psorophora ferox	Psorophora ferox	MF172349.1	100.00%	0.0	99.68%	
Ps_ferox_GF_S110	621	Psorophora ferox	Psorophora ferox	MF172349.1	100.00%	0.0	99.68%	
Ps_ferox_GF_S111	621	Psorophora ferox	Psorophora ferox	MF172347.1	99.00%	0.0	99.51%	
Ur_geometrica_GF_S112	621	Uranotaenia geometrica	Uranotaenia geometrica	NC_044662.1	100.00%	0.0	100.00%	
Ur_geometrica_GF_S113	-	Uranotaenia geometrica	-	-	-	-	-	No COI obtained
Ur_geometrica_GF_S114	621	Uranotaenia geometrica	Uranotaenia geometrica	NC_044662.1	100.00%	0.0	100.00%	
Cx_tritaeniorhynchus_MG_S115	653	Culex tritaeniorhynchus	Culex tritaeniorhynchus	MK861440.1	100.00%	0.0	98.77%	

SOURCE DATA FILES

Figure 3—source data 1. Multiple sequence alignment of 169 28S rRNA sequences from this study and from GenBank (FASTA).

Figure 4—source data 1. Multiple sequence alignment of 122 28S rRNA sequences, including two sequences from *Horreolanus sp.* (FASTA).

Figure 4—source data 2. Multiple sequence alignment of 114 18S rRNA sequences, including two sequences from *Horreolanus sp*. (FASTA).

Figure 5—source data 1. Multiple sequence alignment of 106 COI sequences (FASTA).

REFERENCES

Altschul, S. F., Gish, W., Miller, W., Myers, E. W., & Lipman, D. J. (1990). Basic local alignment search tool. *Journal of Molecular Biology*, *215*(3), 403–410. https://doi.org/10.1016/S0022-2836(05)80360-2

Arctander, P. (1995). Comparison of a mitochondrial gene and a corresponding nuclear pseudogene. *Proceedings of the Royal Society B: Biological Sciences*, *262*(1363), 13–19. https://doi.org/10.1098/rspb.1995.0170

Arunachalam, N., Philip Samuel, P., Hiriyan, J., Thenmozhi, V., & Gajanana, A. (2004). Japanese encephalitis in Kerala, South India: Can Mansonia (Diptera: Culicidae) play a supplemental role in transmission? *Journal of Medical Entomology*, *41*(3), 456–461. https://doi.org/10.1603/0022-2585-41.3.456

Aspen, S., & Savage, H. M. (2003). Polymerase chain reaction assay identifies North American members of the Culex pipiens complex based on nucleotide sequence differences in the acetylcholinesterase gene Ace.2. *Journal of the American Mosquito Control Association*, *19*(4), 323–328.

Auerswald, H., Maquart, P. O., Chevalier, V., & Boyer, S. (2021). Mosquito vector competence for japanese encephalitis virus. *Viruses*, *13*(6), 1154. https://doi.org/10.3390/v13061154

Bankevich, A., Nurk, S., Antipov, D., Gurevich, A. A., Dvorkin, M., Kulikov, A. S., Lesin, V. M., Nikolenko, S. I., Pham, S., Prjibelski, A. D., Pyshkin, A. V., Sirotkin, A. V., Vyahhi, N., Tesler, G., Alekseyev, M. A., & Pevzner, P. A. (2012). SPAdes: A new genome assembly algorithm and its applications to single-cell sequencing. *Journal of Computational Biology*, *19*(5), 455–477.

https://doi.org/10.1089/cmb.2012.0021

Barrio-Nuevo, K. M., Cunha, M. S., Luchs, A., Fernandes, A., Rocco, I. M., Mucci, L. F., DE Souza, R. P., Medeiros-Sousa, A. R., Ceretti-Junior, W., & Marrelli, M. T. (2020). Detection of Zika and dengue viruses in wildcaught mosquitoes collected during field surveillance in an environmental protection area in São Paulo, Brazil. *PLoS ONE*, *15*(10), e0227239. https://doi.org/10.1371/journal.pone.0227239

Batovska, J., Cogan, N. O. I., Lynch, S. E., & Blacket, M. J. (2017). Using next-generation sequencing for DNA barcoding: Capturing allelic variation in ITS2. *G3: Genes, Genomes, Genetics*, *7*(1), 19–29. https://doi.org/10.1534/G3.116.036145/-/DC1

Beebe, N. W. (2018). DNA barcoding mosquitoes: Advice for potential prospectors. *Parasitology*, *145*(5), 622–633. https://doi.org/10.1017/S0031182018000343

Behura, S. K. (2006). Molecular marker systems in insects: current trends and future avenues. *Molecular Ecology*, *15*(11), 3087–3113. https://doi.org/10.1111/J.1365-294X.2006.03014.X

Belda, E., Nanfack-Minkeu, F., Eiglmeier, K., Carissimo, G., Holm, I., Diallo, M., Diallo, D., Vantaux, A., Kim, S., Sharakhov, I. V., & Vernick, K. D. (2019). De novo profiling of RNA viruses in Anopheles malaria vector mosquitoes from forest ecological zones in Senegal and Cambodia. *BMC Genomics*, *20*(1), 664. https://doi.org/10.1186/s12864-019-6034-1

Bhattacharya, S., & Basu, P. (2016). The Southern House Mosquito, Culex quinquefasciatus: profile of a smart vector. *Journal of Entomology and Zoology Studies JEZS*, *4*(2), 73–81.

Bishop-Lilly, K. A., Turell, M. J., Willner, K. M., Butani, A., Nolan, N. M. E., Lentz, S. M., Akmal, A., Mateczun, A., Brahmbhatt, T. N., Sozhamannan, S., Whitehouse, C. A., & Read, T. D. (2010). Arbovirus detection in insect vectors by Rapid, high- throughput pyrosequencing. *PLoS Neglected Tropical Diseases*, *4*(11), e878. https://doi.org/10.1371/journal.pntd.0000878

Brault, A. C., Foy, B. D., Myles, K. M., Kelly, C. L. H., Higgs, S., Weaver, S. C., Olson, K. E., Miller, B. R., & Powers, A. M. (2004). Infection patterns of o'nyong nyong virus in the malaria-transmitting mosquito, Anopheles gambiae. *Insect Molecular Biology*, *13*(6), 625–635. https://doi.org/10.1111/j.0962-1075.2004.00521.x

Cardoso, J. da C., de Almeida, M. A. B., dos Santos, E., da Fonseca, D. F., Sallum, M. A. M., Noll, C. A., Monteiro, H. A. d. O., Cruz, A. C. R., Carvalho, V. L., Pinto, E. V., Castro, F. C., Neto, J. P. N., Segura, M. N. O., & Vasconcelos, P. F. C. (2010). Yellow fever virus in Haemagogus

leucocelaenus and Aedes serratus mosquitoes, Southern Brazil, 2008. *Emerging Infectious Diseases*, *16*(12), 1918–1924. https://doi.org/10.3201/eid1612.100608

Chandler, J. A., Liu, R. M., & Bennett, S. N. (2015). RNA Shotgun Metagenomic Sequencing of Northern California (USA) Mosquitoes Uncovers Viruses, Bacteria, and Fungi. *Frontiers in Microbiology*, *6*, 185. https://doi.org/10.3389/fmicb.2015.00185

Cornel, A. J., Mcabee, R. D., Rasgon, J., Stanich, M. A., Scott, T. W., & Coetzee, M. (2003). Differences in Extent of Genetic Introgression between Sympatric Culex pipiens and Culex quinquefasciatus (Diptera: Culicidae) in California and South Africa. *Journal of Medical Entomology*, *40*(1), 36–51. https://doi.org/10.1603/0022-2585-40.1.36

Danforth, B. N., Lin, C. P., & Fang, J. (2005). How do insect nuclear ribosomal genes compare to protein-coding genes in phylogenetic utility and nucleotide substitution patterns? *Systematic Entomology*, *30*(4), 549–562. https://doi.org/10.1111/J.1a365-3113.2005.00305.X

De Oliveira, C. D., Gonçalves, D. S., Baton, L. A., Shimabukuro, P. H. F., Carvalho, F. D., & Moreira, L. A. (2015). Broader prevalence of Wolbachia in insects including potential human disease vectors. *Bulletin of Entomological Research*, *105*(3), 305–315. https://doi.org/10.1017/S0007485315000085

Desdouits, M., Kamgang, B., Berthet, N., Tricou, V., Ngoagouni, C., Gessain, A., Manuguerra, J. C., Nakouné, E., & Kazanji, M. (2015). Genetic characterization of Chikungunya virus in the Central African Republic. *Infection, Genetics and Evolution*, *33*, 25–31. https://doi.org/10.1016/J.MEEGID.2015.04.006

Diallo, D., Fall, G., Diagne, C. T., Gaye, A., Ba, Y., Dia, I., Faye, O., & Diallo, M. (2020). Concurrent amplification of Zika, chikungunya, and yellow fever virus in a sylvatic focus of arboviruses in Southeastern Senegal, 2015. *BMC Microbiology*, *20*, 181. https://doi.org/10.1186/s12866-020-01866-9

Edgar, R. C. (2004). MUSCLE: A multiple sequence alignment method with reduced time and space complexity. *BMC Bioinformatics*, *5*, 113. https://doi.org/10.1186/1471-2105-5-113

Edwards, F. W. (1941). *Mosquitoes of the Ethiopian Region: III. Culicine Adults and Pupae*. Order of the Trustees.

Farajollahi, A., Fonseca, D. M., Kramer, L. D., & Marm Kilpatrick, A. (2011). “Bird biting” mosquitoes and human disease: A review of the role of Culex pipiens complex mosquitoes in epidemiology.

Infection, Genetics and Evolution, *11*(7), 1577–1585. doi: 10.1016/j.meegid.2011.08.013

Fauver, J. R., Akter, S., Morales, A. I. O., Black, W. C., Rodriguez, A. D., Stenglein, M. D., Ebel, G. D., & Weger-Lucarelli, J. (2019). A reverse-transcription/RNase H based protocol for depletion of mosquito ribosomal RNA facilitates viral intrahost evolution analysis, transcriptomics and pathogen discovery. *Virology*, *528*, 181–197. https://doi.org/10.1016/j.virol.2018.12.020

Foley, D. H., Rueda, L. M., & Wilkerson, R. C. (2007). Insight into Global Mosquito Biogeography from Country Species Records. *Journal of Medical Entomology*, *44*(4), 554–567. https://doi.org/10.1093/JMEDENT/44.4.554

Folmer, O., Black, M., Hoeh, W., Lutz, R., & Vrijenhoek, R. (1994). DNA primers for amplification of mitochondrial cytochrome c oxidase subunit I from diverse metazoan invertebrates. *Molecular Marine Biology and Biotechnology*, *3*(5), 294–299.

Gale, K., & Crampton, J. (1989). The ribosomal genes of the mosquito, Aedes aegypti. *European Journal of Biochemistry*, *185*(2), 311–317. https://doi.org/10.1111/j.1432-1033.1989.tb15117.x

Grjebine, A. (1966). *Insectes Diptères Culicidae Anophelinae*. ORSTOM / CNRS.

Hajibabaei, M., Singer, G. A. C., & Hickey, D. A. (2006). Benchmarking DNA barcodes: An assessment using available primate sequences. *Genome*, *49*(7), 851–854. https://doi.org/10.1139/G06-025/SUPPL_FILE/G06-025B.PDF

Halstead, S. B. (2019). Travelling arboviruses: A historical perspective. *Travel Medicine and Infectious Disease*, *31*, 101471. https://doi.org/10.1016/J.TMAID.2019.101471

Harbach, R. E. (2007). The Culicidae (Diptera): A review of taxonomy, classification and phylogeny. *Zootaxa*, *1668*(1), 591–638. https://doi.org/10.11646/zootaxa.1668.1.28

Harbach, R. E., Culverwell, C. L., & Kitching, I. J. (2017). Phylogeny of the nominotypical subgenus of Culex (Diptera: Culicidae): insights from analyses of anatomical data into interspecific relationships and species groups in an unresolved tree. *Systematics and Biodiversity*, *15*(4), 296–306. https://doi.org/10.1080/14772000.2016.1252439

Harbach, R. E., & Kitching, I. J. (2016). The phylogeny of Anophelinae revisited: Inferences about the origin and classification of Anopheles (Diptera: Culicidae). *Zoologica Scripta*, *45*(1), 34–47. https://doi.org/10.1111/zsc.12137

Hayes, C. G., Basit, A., Bagar, S., & Akhter, R. (1980). Vector competence of Culex tritaeniorhynchus (Diptera: Culicidae) for West Nile virus. *Journal of Medical Entomology*.

https://doi.org/10.1093/jmedent/17.2.172

Hebert, P. D. N., Cywinska, A., Ball, S. L., & DeWaard, J. R. (2003). Biological identifications through DNA barcodes. *Proceedings of the Royal Society B: Biological Sciences*, *270*(1512), 313–321. https://doi.org/10.1098/rspb.2002.2218

Héraud, J.-M., Andriamandimby, S. F., Olive, M.-M., Guis, H., Miatrana Rasamoelina, V., & Tantely, L. (2022). Arthropod-Borne Viruses of Madagascar. In S. M. Goodman (Ed.), *The New Natural History of Madagascar* (pp. 285–291). Princeton University Press.

Hoyos-López, R., Soto, S. U., Rúa-Uribe, G., & Gallego-Gómez, J. C. (2015). Molecular identification of saint louis encephalitis virus genotype IV in Colombia. *Memorias Do Instituto Oswaldo Cruz*, *110*(6), 719–725. https://doi.org/10.1590/0074-02760280040

Huang, Y., & Ward, R. A. (1981). A Pictorial Key for the Identification of the Mosquitoes Associated with Yellow Fever in Africa. *Mosquito Systematics*.

Hurst, G. D. D., & Jiggins, F. M. (2005). Problems with mitochondrial DNA as a marker in population, phylogeographic and phylogenetic studies: The effects of inherited symbionts. *Proceedings of the Royal Society B: Biological Sciences*, *272*, 1525–1534. https://doi.org/10.1098/rspb.2005.3056

Jacobi, J. C., & Serie, C. (1972). Prevalence of group B arbovirus infections in French Guiana in 1967-69. *Medecine d'Afrique Noire*, *19*(3), 225–226.

Jupp, P. G., Kemp, A., Grobbelaar, A., Leman, P., Burt, F. J., Alahmed, A. M., Al Mujalli, D., Al Khamees, M., & Swanepoel, R. (2002). The 2000 epidemic of Rift Valley fever in Saudi Arabia: Mosquito vector studies. *Medical and Veterinary Entomology*. https://doi.org/10.1046/j.1365-2915.2002.00371.x

Kim, H., Cha, G. W., Jeong, Y. E., Lee, W. G., Chang, K. S., Roh, J. Y., Yang, S. C., Park, M. Y., Park, C., & Shin, E. H. (2015). Detection of Japanese encephalitis virus genotype V in Culex orientalis and Culex pipiens (Diptera: Culicidae) in Korea. *PLoS ONE*, *10*(2), e0116547. https://doi.org/10.1371/journal.pone.0116547

Kraemer, M. U. G., Reiner, R. C., Brady, O. J., Messina, J. P., Gilbert, M., Pigott, D. M., Yi, D., Johnson, K., Earl, L., Marczak, L. B., Shirude, S., Davis Weaver, N., Bisanzio, D., Perkins, T. A., Lai, S., Lu, X., Jones, P., Coelho, G. E., Carvalho, R. G., … Golding, N. (2019). Past and future spread of the arbovirus vectors Aedes aegypti and Aedes albopictus. *Nature Microbiology*, *4*(5),

854–863. https://doi.org/10.1038/s41564-019-0376-y

Kukutla, P., Steritz, M., & Xu, J. (2013). Depletion of ribosomal RNA for mosquito gut metagenomic RNA-seq. *Journal of Visualized Experiments*, *74*, 50093. https://doi.org/10.3791/50093

Kumar, N., Creasy, T., Sun, Y., Flowers, M., Tallon, L. J., & Dunning Hotopp, J. C. (2012). Efficient subtraction of insect rRNA prior to transcriptome analysis of Wolbachia-Drosophila lateral gene transfer. *BMC Research Notes*, *5*, 230. https://doi.org/10.1186/1756-0500-5-230

Kumar, S., Stecher, G., Li, M., Knyaz, C., & Tamura, K. (2018). MEGA X: Molecular evolutionary genetics analysis across computing platforms. *Molecular Biology and Evolution*, *35*(6), 1547–1549. https://doi.org/10.1093/molbev/msy096

Logue, K., Chan, E. R., Phipps, T., Small, S. T., Reimer, L., Henry-Halldin, C., Sattabongkot, J., Siba, P. M., Zimmerman, P. A., & Serre, D. (2013). Mitochondrial genome sequences reveal deep divergences among Anopheles punctulatus sibling species in Papua New Guinea. *Malaria Journal*, *12*(1), 1–11. https://doi.org/10.1186/1475-2875-12-64/FIGURES/3

Lorenz, C., Alves, J. M. P., Foster, P. G., Suesdek, L., & Sallum, M. A. M. (2021). Phylogeny and temporal diversification of mosquitoes (Diptera: Culicidae) with an emphasis on the Neotropical fauna. *Systematic Entomology*, *46*(4), 798–811. https://doi.org/10.1111/SYEN.12489

Lutomiah, J., Bast, J., Clark, J., Richardson, J., Yalwala, S., Oullo, D., Mutisya, J., Mulwa, F., Musila, L., Khamadi, S., Schnabel, D., Wurapa, E., & Sang, R. (2013). Abundance, diversity, and distribution of mosquito vectors in selected ecological regions of Kenya: Public health implications. *Journal of Vector Ecology*, *38*(1), 134–142. https://doi.org/10.1111/j.1948-7134.2013.12019.x

Madeira, F., Park, Y. M., Lee, J., Buso, N., Gur, T., Madhusoodanan, N., Basutkar, P., Tivey, A. R. N., Potter, S. C., Finn, R. D., & Lopez, R. (2019). The EMBL-EBI search and sequence analysis tools APIs in 2019. *Nucleic Acids Research*, *47*(W1), W636–W641. https://doi.org/10.1093/nar/gkz268

Maquart, P. O., & Boyer, S. (2022). Culex vishnui. *Trends in Parasitology*, *Vector of the Month*, 491–492. https://doi.org/10.1016/J.PT.2022.01.003

Maquart, P. O., Sokha, C., & Boyer, S. (2021). Mosquito diversity (Diptera: Culicidae) and medical importance, in a bird sanctuary inside the flooded forest of Prek Toal, Cambodia. *Journal of Asia-Pacific Entomology*, *24*(4), 1221–1227. https://doi.org/10.1016/j.aspen.2021.08.001

Mitchell, C. J., Forattini, O. P., & Miller, B. R. (1986). Vector competence experiments with Rocio virus and three mosquito species from the epidemic zone in Brazil. *Revista de Saúde Pública*, *20*(3), 171–177. https://doi.org/10.1590/s0034-89101986000300001

Morlan, J. D., Qu, K., & Sinicropi, D. V. (2012). Selective depletion of rRNA enables whole transcriptome profiling of archival fixed tissue. *PLoS ONE*, *7*(8), e42882. https://doi.org/10.1371/journal.pone.0042882

Mukwaya, L. G., Kayondo, J. K., Crabtree, M. B., Savage, H. M., Biggerstaff, B. J., & Miller, B. R. (2000). Genetic differentiation in the yellow fever virus vector, Aedes simpsoni complex, in Africa: Sequence variation in the ribosomal DNA internal transcribed spacers of anthropophilic and non-anthropophilic populations. *Insect Molecular Biology*, *9*(1), 85–91. doi: 10.1046/j.1365-2583.2000.00161.x

Mwangangi, J. M., Muturi, E. J., Muriu, S. M., Nzovu, J., Midega, J. T., & Mbogo, C. (2013). The role of Anopheles arabiensis and Anopheles coustani in indoor and outdoor malaria transmission in Taveta District, Kenya. *Parasites and Vectors*, *6*, 114. https://doi.org/10.1186/1756-3305-6-114

Navarro, J. C., & Weaver, S. C. (2004). Molecular phylogeny of the Vomerifer and Pedroi Groups in the spissipes section of the subgenus Culex (Melanoconion). *Journal of Medical Entomology*, *41*(4), 575–581. https://doi.org/10.1603/0022-2585-41.4.575

Nchoutpouen, E., Talipouo, A., Djiappi-Tchamen, B., Djamouko-Djonkam, L., Kopya, E., Ngadjeu, C. S., Doumbe-Belisse, P., Awono-Ambene, P., Kekeunou, S., Wondji, C. S., & Antonio-Nkondjio, C. (2019). Culex species diversity, susceptibility to insecticides and role as potential vector of Lymphatic filariasis in the city of Yaoundé, Cameroon. *PLoS Neglected Tropical Diseases*, *13*(4), e0007229. https://doi.org/10.1371/journal.pntd.0007229

Ndiaye, E. H., Fall, G., Gaye, A., Bob, N. S., Talla, C., Diagne, C. T., Diallo, D., Ba, Y., Dia, I., Kohl, A., Sall, A. A., & Diallo, M. (2016). Vector competence of Aedes vexans (Meigen), Culex poicilipes (Theobald) and Cx. quinquefasciatus Say from Senegal for West and East African lineages of Rift Valley fever virus. *Parasites and Vectors*, *9*, 94. https://doi.org/10.1186/s13071-016-1383-y

Nepomichene, T. N. J. J., Raharimalala, F. N., Andriamandimby, S. F., Ravalohery, J. P., Failloux, A. B., Heraud, J. M., & Boyer, S. (2018). Vector competence of Culex antennatus and Anopheles coustani mosquitoes for Rift Valley fever virus in Madagascar. *Medical and Veterinary*

Entomology, *32*(2), 259–262. https://doi.org/10.1111/mve.12291

Nikolay, B., Diallo, M., Boye, C. S. B., & Sall, A. A. (2011). Usutu virus in Africa. *Vector-Borne and Zoonotic Diseases*, *11*(11), 1417–1423. https://doi.org/10.1089/vbz.2011.0631

Oo, T. T., Kaiser, A., & Becker, N. (2006). Illustrated keys to the anopheline mosquitoes of Myanmar. *Journal of Vector Ecology*, *31*(1), 9–16. https://doi.org/10.3376/1081-1710(2006)31[9:ikttam]2.0.co;2

Pereira Serra, O., Fernandes Cardoso, B., Maria Ribeiro, A. L., dos Santos, F. A. L., & Dezengrini Slhessarenko, R. (2016). Mayaro virus and dengue virus 1 and 4 natural infection in culicids from Cuiabá, state of Mato Grosso, Brazil. *Memórias Do Instituto Oswaldo Cruz*, *111*(1), 20–29. https://doi.org/10.1590/0074-02760150270

Phelps, W. A., Carlson, A. E., & Lee, M. T. (2021). Optimized design of antisense oligomers for targeted rRNA depletion. *Nucleic Acids Research*, *49*(1), e5. https://doi.org/10.1093/nar/gkaa1072

Quast, C., Pruesse, E., Yilmaz, P., Gerken, J., Schweer, T., Yarza, P., Peplies, J., & Glöckner, F. O. (2013). The SILVA ribosomal RNA gene database project: Improved data processing and web-based tools. *Nucleic Acids Research*, *41*(Database issue), D590–D596. https://doi.org/10.1093/nar/gks1219

Ratnasingham, S., & Hebert, P. D. N. (2007). BOLD: The Barcode of Life Data System: Barcoding. *Molecular Ecology Notes*, *7*(3), 355–364. https://doi.org/10.1111/j.1471-8286.2007.01678.x

Ratovonjato, J., Olive, M. M., Tantely, L. M., Andrianaivolambo, L., Tata, E., Razainirina, J., Jeanmaire, E., Reynes, J. M., & Elissa, N. (2011). Detection, isolation, and genetic characterization of Rift Valley fever virus from anopheles (Anopheles) coustani, anopheles (Anopheles) squamosus, and culex (Culex) antennatus of the haute matsiatra region, Madagascar. *Vector-Borne and Zoonotic Diseases*, *11*(6), 753–759. https://doi.org/10.1089/vbz.2010.0031

Ratsitorahina, M., Harisoa, J., Ratovonjato, J., Biacabe, S., Reynes, J. M., Zeller, H., Raoelina, Y., Talarmin, A., Richard, V., & Soares, J. L. (2008). Outbreak of dengue and chikungunya fevers, Toamasina, Madagascar, 2006. *Emerging Infectious Diseases*, *14*(7), 1135–1137. https://doi.org/10.3201/EID1407.071521

Rattanarithikul, R., Harbach, R. E., Harrison, B. A., Panthusiri, P., & Coleman, R. E. (2007). Illustrated

968 keys to the mosquitoes of Thailand V. Genera Orthopodomyia, Kimia, Malaya, Topomyia,
969 Tripteroides, and Toxorhynchites. *Suppl 1*, *38*(Suppl 2), 1–65.
970 Rattanarithikul, R., Harbach, R. E., Harrison, B. A., Panthusiri, P., Coleman, R. E., & Richardson, J. H.
971 (2010). Illustrated keys to the mosquitoes of Thailand. VI. Tribe Aedini. *Southeast Asian Journal*
972 *of Tropical Medicine and Public Health*, *41*(Suppl 1), 1–225.
973 Rattanarithikul, R., Harbach, R. E., Harrison, B. A., Panthusiri, P., Jones, J. W., & Coleman, R. E.
974 (2005). Illustrated keys to the mosquitoes of Thailand. II. Genera Culex and Lutzia. *The*
975 *Southeast Asian Journal of Tropical Medicine and Public Health*.
976 Rattanarithikul, R., Harrison, B. A., Harbach, R. E., Panthusiri, P., & Coleman, R. E. (2006). Illustrated
977 keys to the mosquitoes of Thailand IV. Anopheles. *Southeast Asian Journal of Tropical Medicine*
978 *and Public Health*, *37*(Suppl 2), 1–26.
979 Rattanarithikul, R., Harrison, B. A., Panthusiri, P., & Coleman, R. E. (2005). Illustrated keys to the
980 mosquitoes of Thailand I. Background; geographic distribution; lists of genera, subgenera, and
981 species; and a key to the genera. *Southeast Asian Journal of Tropical Medicine and Public*
982 *Health*, *36*(Suppl 1), 1–80.
983 Rattanarithikul, R., Harrison, B. A., Panthusiri, P., Peyton, E. L., & Coleman, R. E. (2006). Illustrated
984 keys to the mosquitoes of Thailand: III. Genera Aedeomyia, Ficalbia, Mimomyia, Hodgesia,
985 Coquillettidia, Mansonia, and Uranotaenia. *Southeast Asian Journal of Tropical Medicine and*
986 *Public Health*, *37*(Suppl 1), 1–10.
987 Rausch, T., Fritz, M. H. Y., Untergasser, A., & Benes, V. (2020). Tracy: Basecalling, alignment,
988 assembly and deconvolution of sanger chromatogram trace files. *BMC Genomics*, *21*(1), 230.
989 https://doi.org/10.1186/s12864-020-6635-8
990 Rausch, T., Hsi-Yang Fritz, M., Korbel, J. O., & Benes, V. (2019). Alfred: Interactive multi-sample
991 BAM alignment statistics, feature counting and feature annotation for long- and short-read
992 sequencing. *Bioinformatics*, *35*(14), 2489–2491. https://doi.org/10.1093/bioinformatics/bty1007
993 Reidenbach, K. R., Cook, S., Bertone, M. A., Harbach, R. E., Wiegmann, B. M., & Besansky, N. J.
994 (2009). Phylogenetic analysis and temporal diversification of mosquitoes (Diptera: Culicidae)
995 based on nuclear genes and morphology. *BMC Evolutionary Biology*, *9*(1), 1–14.
996 https://doi.org/10.1186/1471-2148-9-298/FIGURES/4
997 Romero-Alvarez, D., & Escobar, L. E. (2018). Oropouche fever, an emergent disease from the

998 Americas. *Microbes and Infection*, *20*(3), 135–146.
999 https://doi.org/10.1016/J.MICINF.2017.11.013
1000 Rueda, L. M. (2004). Pictorial keys for the identification of mosquitoes (Diptera: Culicidae) associated
1001 with Dengue Virus Transmission. *Zootaxa*. https://doi.org/10.11646/zootaxa.589.1.1
1002 Ruzzante, L., Reijnders, M. J. M. F., & Waterhouse, R. M. (2019). Of Genes and Genomes: Mosquito
1003 Evolution and Diversity. *Trends in Parasitology*, *35*(1), 32–51.
1004 https://doi.org/10.1016/J.PT.2018.10.003/ATTACHMENT/B9BE6BC5-D73A-4FEF-A654-
1005 CC1374C59925/MMC1.MP4
1006 Sallum, M. A. M., & Forattini, O. P. (1996). Revision of the Spissipes Section of Culex (Melanoconion)
1007 (diptera: Culicidae). *Journal of the American Mosquito Control Association*, *12*(3), 517–600.
1008 Saluzzo, J. F., Evidera, T. V., Veas, F., & Gonzalez, J.-P. J. (2018). *Arbovirus Discovery in Central*
1009 *African Republic (1973-1993): Zika, Bozo, Bouboui, and More*.
1010 https://www.researchgate.net/publication/321587457
1011 Sirivanakarn, S. (1982). A review of the Systematics and a Proposed Scheme of Internal
1012 Classification of the New World Subgenus Melanoconion of Culex (Diptera, Culicidae). *Mosquito*
1013 *Systematics*, *14*(4), 265–333.
1014 Stevenson, J. C., Simubali, L., Mbambara, S., Musonda, M., Mweetwa, S., Mudenda, T., Pringle, J.
1015 C., Jones, C. M., & Norris, D. E. (2016). Detection of plasmodium falciparum infection in
1016 anopheles squamosus (diptera: Culicidae) in an area targeted for malaria elimination, Southern
1017 Zambia. *Journal of Medical Entomology*, *53*(6), 1482–1487. https://doi.org/10.1093/jme/tjw091
1018 Sun, L., Li, T. J., Fu, W. B., Yan, Z. T., Si, F. L., Zhang, Y. J., Mao, Q. M., Demari-Silva, B., & Chen,
1019 B. (2019). The complete mt genomes of Lutzia halifaxia, Lt. fuscanus and Culex pallidothorax
1020 (Diptera: Culicidae) and comparative analysis of 16 Culex and Lutzia mt genome sequences.
1021 *Parasites and Vectors*, *12*, 368. https://doi.org/10.1186/s13071-019-3625-2
1022 Tabue, R. N., Awono-Ambene, P., Etang, J., Atangana, J., Antonio-Nkondjio, C., Toto, J. C.,
1023 Patchoke, S., Leke, R. G. F., Fondjo, E., Mnzava, A. P., Knox, T. B., Tougordi, A., Donnelly, M.
1024 J., & Bigoga, J. D. (2017). Role of Anopheles (Cellia) rufipes (Gough, 1910) and other local
1025 anophelines in human malaria transmission in the northern savannah of Cameroon: a cross-
1026 sectional survey. *Parasites and Vectors*, *10*(1), 1–11. https://doi.org/10.1186/S13071-016-1933-
1027 3/FIGURES/6

Takhampunya, R., Kim, H. C., Tippayachai, B., Kengluecha, A., Klein, T. A., Lee, W. J., Grieco, J., & Evans, B. P. (2011). Emergence of Japanese encephalitis virus genotype v in the Republic of Korea. *Virology Journal*, *8*, 449. https://doi.org/10.1186/1743-422X-8-449

Talaga, S., Duchemin, J. B., Girod, R., & Dusfour, I. (2021). The Culex Mosquitoes (Diptera: Culicidae) of French Guiana: A Comprehensive Review With the Description of Three New Species. *Journal of Medical Entomology*, *58*(1), 182–221. https://doi.org/10.1093/JME/TJAA205

Thongsripong, P., Chandler, J. A., Kittayapong, P., Wilcox, B. A., Kapan, D. D., & Bennett, S. N. (2021). Metagenomic shotgun sequencing reveals host species as an important driver of virome composition in mosquitoes. *Scientific Reports*, *11*(1), 8448. https://doi.org/10.1038/s41598-021-87122-0

Torres-Gutierrez, C., Bergo, E. S., Emerson, K. J., de Oliveira, T. M. P., Greni, S., & Sallum, M. A. M. (2016). Mitochondrial COI gene as a tool in the taxonomy of mosquitoes Culex subgenus Melanoconion. *Acta Tropica*, *164*, 137–149. https://doi.org/10.1016/j.actatropica.2016.09.007

Torres-Gutierrez, C., De Oliveira, T. M. P., Emerson, K. J., Bergo, E. S., & Sallum, M. A. M. (2018). Molecular phylogeny of Culex subgenus Melanoconion (Diptera: Culicidae) based on nuclear and mitochondrial protein-coding genes. *Royal Society Open Science*, *5*, 171900. https://doi.org/10.1098/rsos.171900

Travassos Da Rosa, J. F., De Souza, W. M., De Paula Pinheiro, F., Figueiredo, M. L., Cardoso, J. F., Acrani, G. O., & Teixeira Nunes, M. R. (2017). Oropouche Virus: Clinical, Epidemiological, and Molecular Aspects of a Neglected Orthobunyavirus. *The American Journal of Tropical Medicine and Hygiene*, *96*(5), 1019. https://doi.org/10.4269/AJTMH.16-0672

Turell, M. J., O'guinn, M. L., Dohm, D., Zyzak, M., Watts, D., Fernandez, R., Calampa, C., Klein, T. A., & Jones, J. W. (2008). Susceptibility of Peruvian Mosquitoes to Eastern Equine Encephalitis Virus. *Journal of Medical Entomology*, *45*(4), 720–725. https://doi.org/10.1093/JMEDENT/45.4.720

Turell, Michael J. (1999). Vector competence of three Venezuelan mosquitoes (Diptera: Culicidae) for an epizootic IC strain of Venezuelan equine encephalitis virus. *Journal of Medical Entomology*, *36*(4), 407–409. https://doi.org/10.1093/jmedent/36.4.407

Ughasi, J., Bekard, H. E., Coulibaly, M., Adabie-Gomez, D., Gyapong, J., Appawu, M., Wilson, M. D., & Boakye, D. A. (2012). Mansonia africana and Mansonia uniformis are Vectors in the

transmission of Wuchereria bancrofti lymphatic filariasis in Ghana. *Parasites and Vectors*, *5*(1), 1–5. https://doi.org/10.1186/1756-3305-5-89

Valentine, M. J., Murdock, C. C., & Kelly, P. J. (2019). Sylvatic cycles of arboviruses in non-human primates. *Parasites and Vectors*, *12*(1), 1–18. https://doi.org/10.1186/S13071-019-3732-0/TABLES/4

Vasconcelos, P. F. C., Costa, Z. G., Travassos da Rosa, E. S., Luna, E., Rodrigues, S. G., Barros, V. L. R. S., Dias, J. P., Monteiro, H. A. O., Oliva, O. F. P., Vasconcelos, H. B., Oliveira, R. C., Sousa, M. R. S., Barbosa Da Silva, J., Cruz, A. C. R., Martins, E. C., & Travassos Da Rosa, J. F. S. (2001). Epidemic of jungle yellow fever in Brazil, 2000: Implications of climatic alterations in disease spread. *Journal of Medical Virology*, *65*(3), 598–604. https://doi.org/10.1002/jmv.2078.abs

Vázquez González, A., Ruiz, S., Herrero, L., Moreno, J., Molero, F., Magallanes, A., Sánchez-Seco, M. P., Figuerola, J., & Tenorio, A. (2011). West Nile and Usutu viruses in mosquitoes in Spain, 2008-2009. *American Journal of Tropical Medicine and Hygiene*, *85*(1), 178–181. https://doi.org/10.4269/ajtmh.2011.11-0042

Vezenegho, S. B., Issaly, J., Carinci, R., Gaborit, P., Girod, R., Dusfour, I., & Briolant, S. (2022). Discrimination of 15 Amazonian Anopheline Mosquito Species by Polymerase Chain Reaction—Restriction Fragment Length Polymorphism. *Journal of Medical Entomology*, *59*(3), 1060–1064. https://doi.org/10.1093/JME/TJAC008

Weaver, S. C., Ferro, C., Barrera, R., Boshell, J., & Navarro, J. C. (2004). Venezuelan Equine Encephalitis. *Annual Review of Entomology*, *49*, 141–174. https://doi.org/10.1146/annurev.ento.49.061802.123422

Webster, J. P., Gower, C. M., Knowles, S. C. L., Molyneux, D. H., & Fenton, A. (2016). One health - an ecological and evolutionary framework for tackling Neglected Zoonotic Diseases. *Evolutionary Applications*, *9*(2), 313–333. https://doi.org/10.1111/eva.12341

Weedall, G. D., Irving, H., Hughes, M. A., & Wondji, C. S. (2015). Molecular tools for studying the major malaria vector Anopheles funestus: Improving the utility of the genome using a comparative poly(A) and Ribo-Zero RNAseq analysis. *BMC Genomics*, *16*(1), 931. https://doi.org/10.1186/s12864-015-2114-z

WHO. (2017). Global vector control response 2017–2030. In *World Health Organization*.

1088 Zakrzewski, M., Rašić, G., Darbro, J., Krause, L., Poo, Y. S., Filipović, I., Parry, R., Asgari, S., Devine,
1089 G., & Suhrbier, A. (2018). Mapping the virome in wild-caught Aedes aegypti from Cairns and
1090 Bangkok. *Scientific Reports*, *8*(1), 4690. https://doi.org/10.1038/s41598-018-22945-y
1091 Zeller, H., Van Bortel, W., & Sudre, B. (2016). Chikungunya: Its History in Africa and Asia and Its
1092 Spread to New Regions in 2013–2014. *The Journal of Infectious Diseases*, *214*(suppl_5), S436–
1093 S440. https://doi.org/10.1093/INFDIS/JIW391
1094 Zittra, C., Flechl, E., Kothmayer, M., Vitecek, S., Rossiter, H., Zechmeister, T., & Fuehrer, H. P.
1095 (2016). Ecological characterization and molecular differentiation of Culex pipiens complex taxa
1096 and Culex torrentium in eastern Austria. *Parasites and Vectors*, *9*, 197.
1097 https://doi.org/10.1186/s13071-016-1495-4
1098

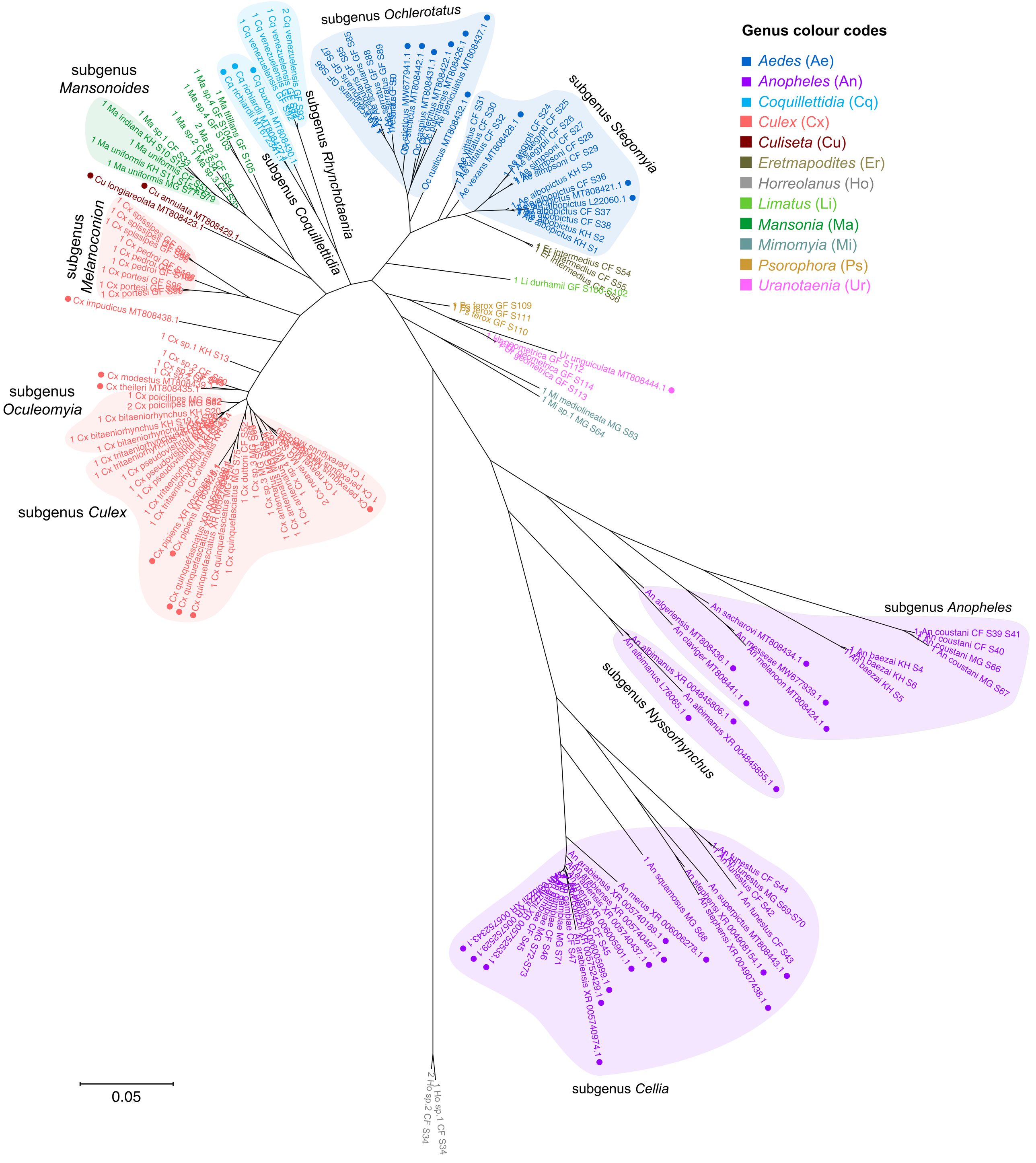
Genus colour codes
Aedes (Ae)
Anopheles (An)
Coquillettidia (Cq)
Culex (Cx)
Culiseta (Cu)
Eretmapodites (Er)
Horreolanus (Ho)
Limatus (Li)
Mansonia (Ma)
Mimomyia (Mi)
Psorophora (Ps)
Uranotaenia (Ur)
subgenus Mansonoides
subgenus Ochlerotatus
subgenus Rhynchotaenia
subgenus Coquillettidia
subgenus Stegomyia
subgenus Melanoconion
subgenus Oculeomyia
subgenus Culex
subgenus Anopheles
subgenus Nyssorhynchus
subgenus Cellia
0.05